Introduction to Receiver Functions

I. Definition of a Receiver Function
II. Slant Stacking
III. Modeling of Receiver Functions
IV. S-wave Receiver Functions

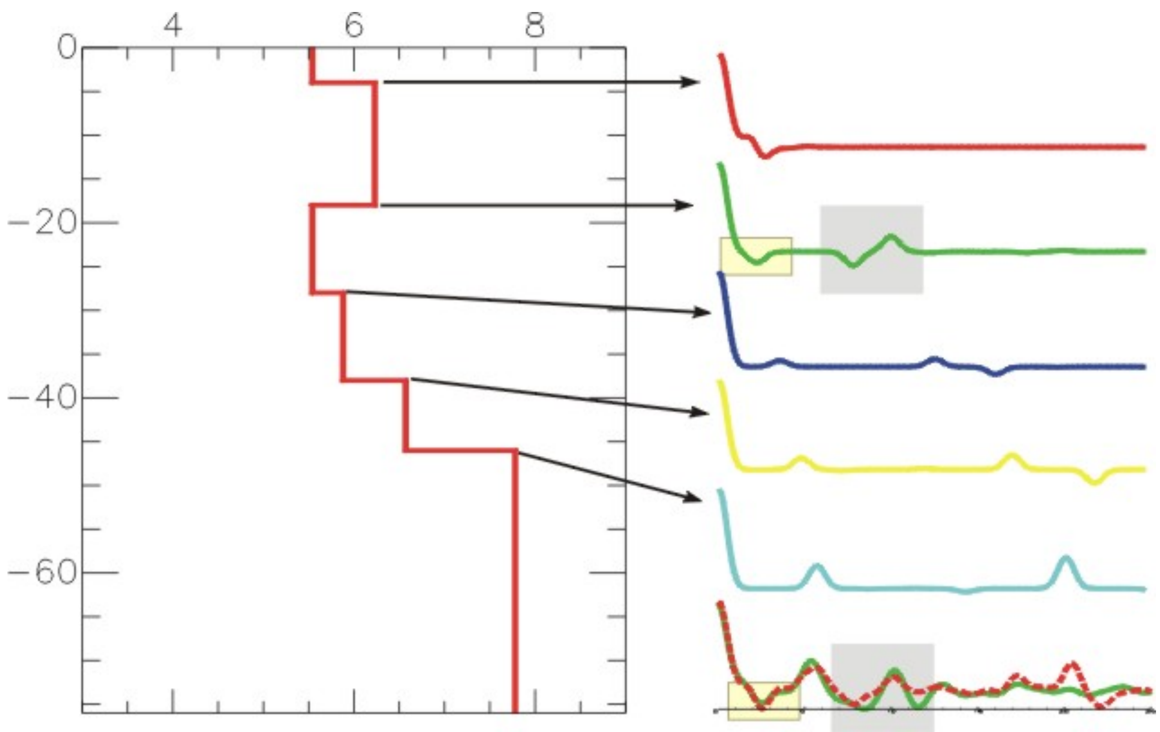

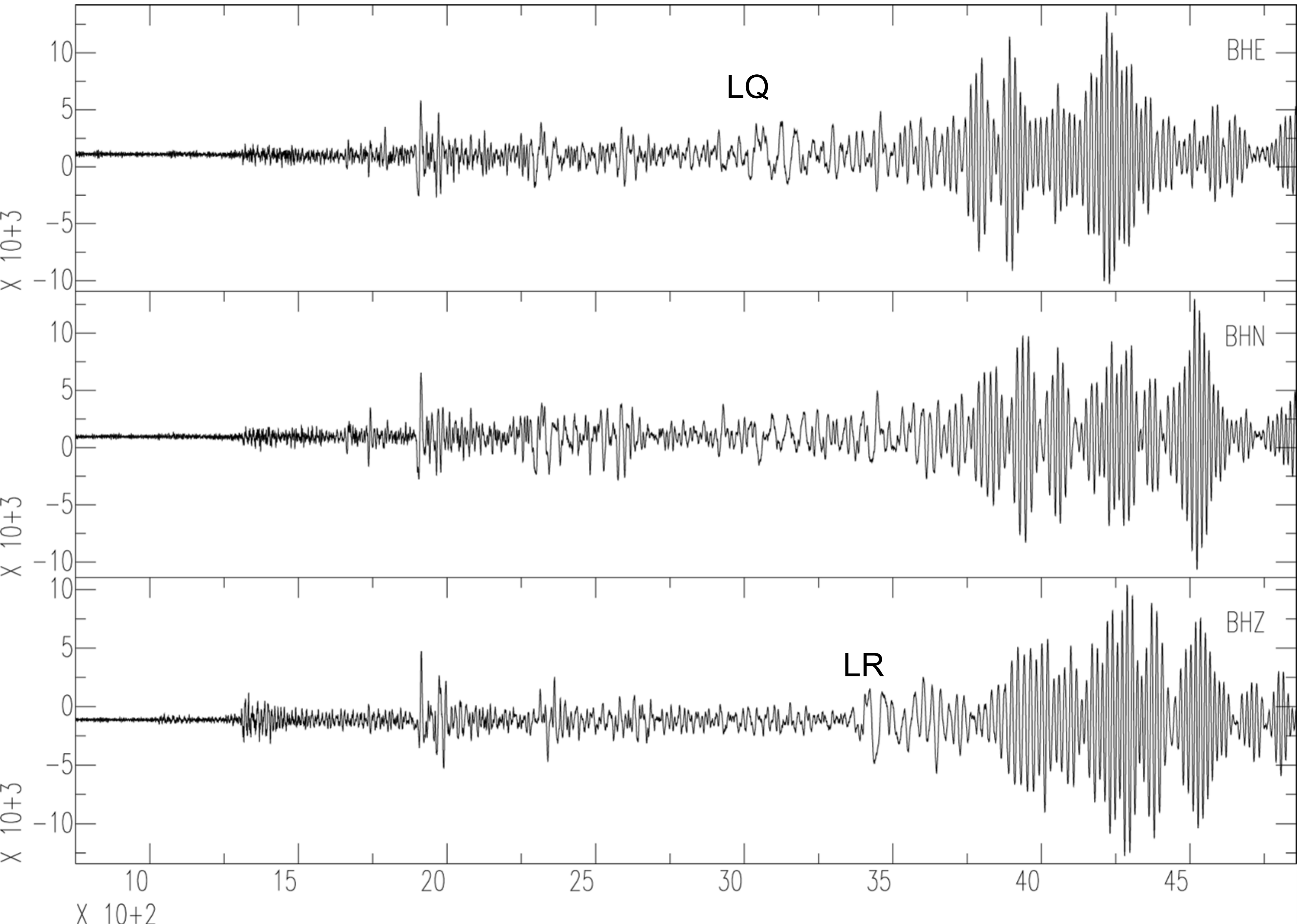

BHE
LQ
BHN
BHZ
LR
X 10+3
X 10+2

Body Waves
P and S waves Particle Motion

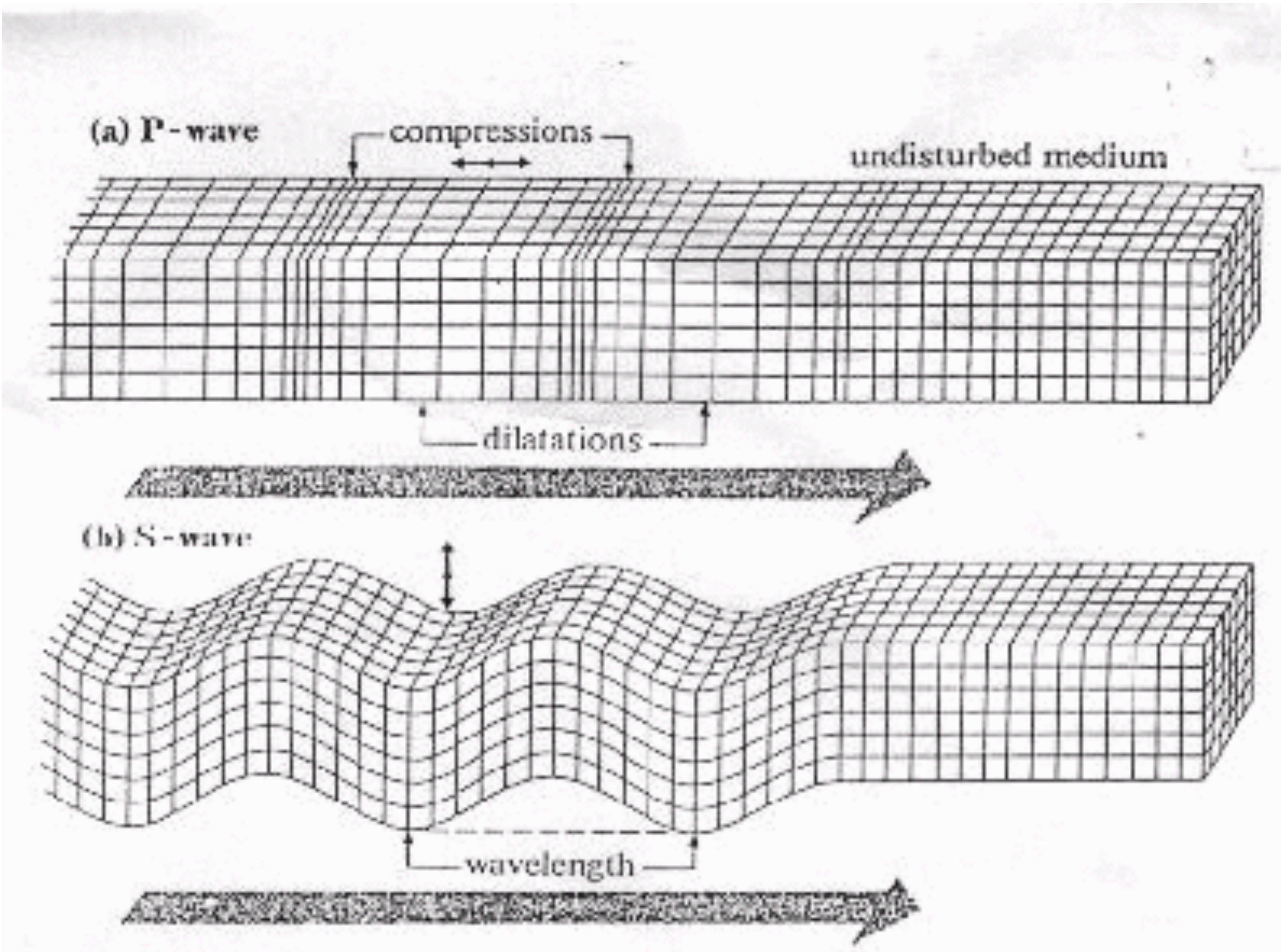

Body Waves: Polarization

P, SV, and SH :

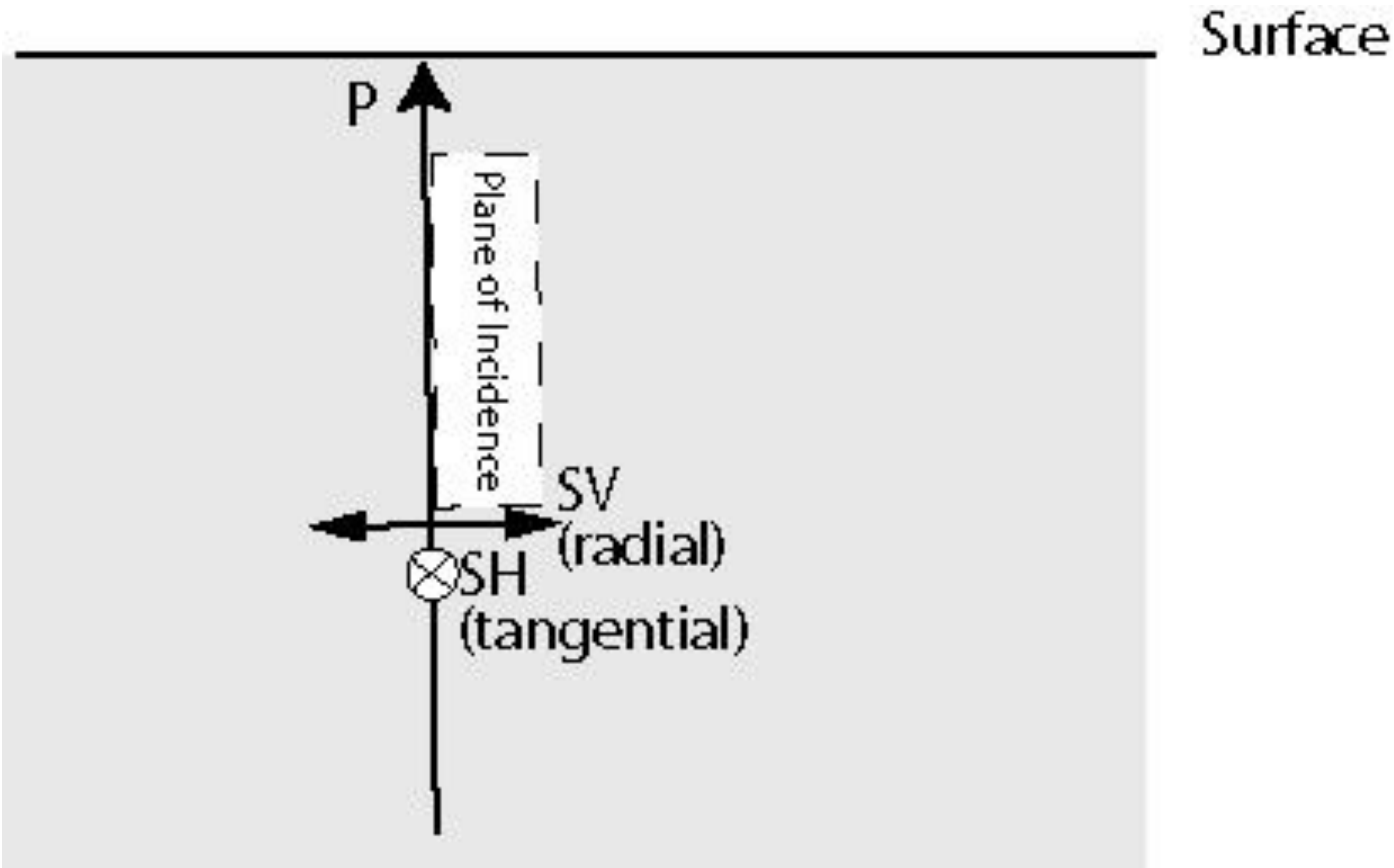

Seismic Body Waves

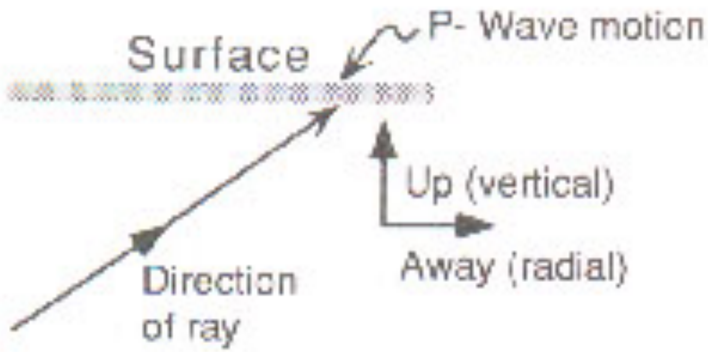

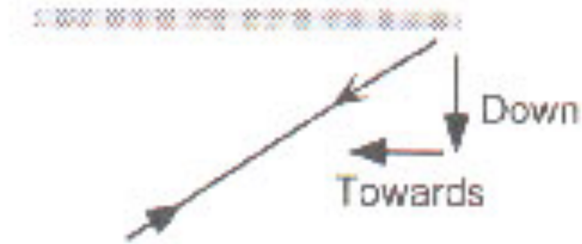

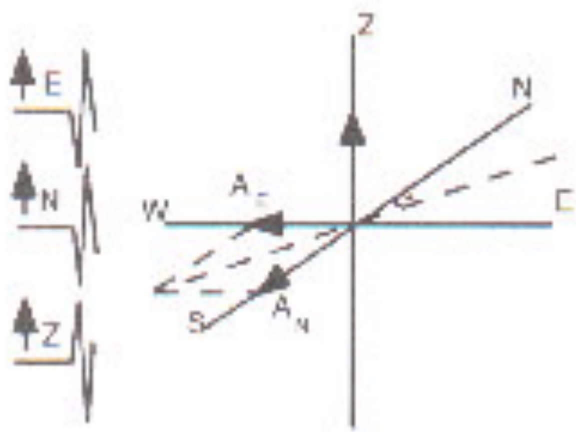

Receiver Functions

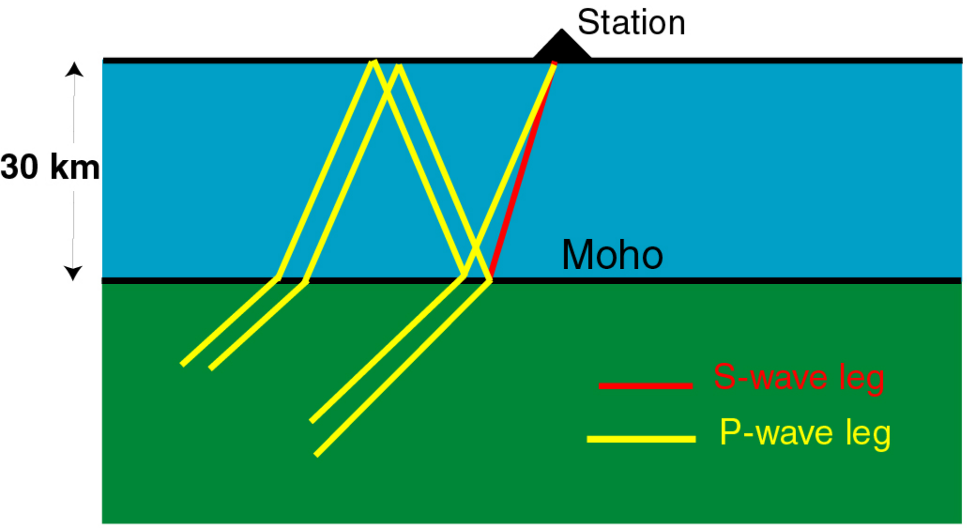

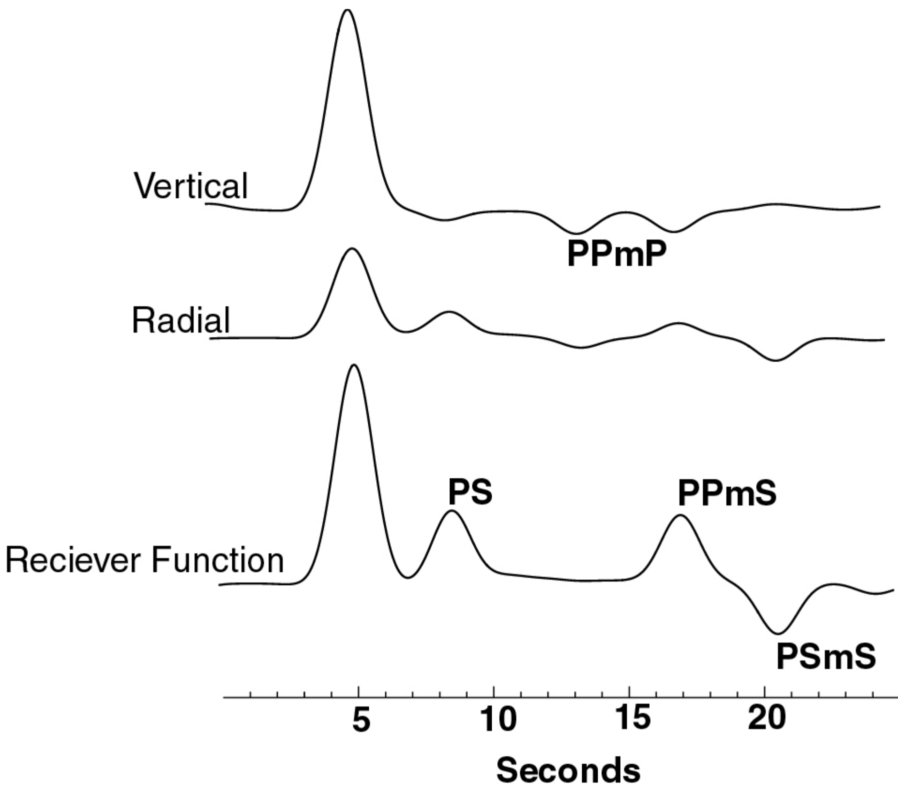

$$R(\omega) = \frac{U_R(\omega)}{U_V(\omega)} = \frac{I(\omega)\cdot S(\omega)\cdot E_R{}^R(\omega)\cdot E_R{}^S(\omega)}{I(\omega)\cdot S(\omega)\cdot E_V{}^R(\omega)\cdot E_V{}^S(\omega)}$$

$$= \frac{E_R{}^R(\omega)\cdot E_R{}^S(\omega)}{E_V{}^R(\omega)\cdot E_V{}^S(\omega)} \cong \frac{E_R{}^R(\omega)}{E_V{}^R(\omega)}$$

Fundamental Assumptions

- Plane Wave Approximation
- The PS is primarily recorded on the radial (the vertical component is negligible)

- These assumptions lead to the result that the receiver function *only* includes P-to-S converted energy

$$\hat{z}_k = \frac{z_k}{z_0}, \hat{r}_k = \frac{r_k}{r_0}$$

$$E_R(\omega) = r_0\left[1 + \hat{r}_p e^{-i\omega t_p} + \hat{r}_{ps} e^{-i\omega t_{ps}}\right]$$

$$E_Z(\omega) = z_0\left[1 + \hat{z}_p e^{-i\omega t_p} + \hat{z}_{ps} e^{-i\omega t_{ps}}\right]$$

we can assume $z_{ps} << 1$

$$R(\omega) = \frac{r_0}{z_0} \frac{1 + \hat{r}_p e^{-i\omega t_p} + \hat{r}_{ps} e^{-i\omega t_{ps}}}{1 + \hat{z}_p e^{-i\omega t_p}}$$

using the binomial expansion : $(1 + \mathrm{x})^{-1} = 1 - x + x^2 + \ldots$

$$\mathrm{R}(\omega) \cong \frac{r_0}{z_0}\left(1 - \hat{z}_p e^{-i\omega t_p}\right)\left(1 + \hat{r}_p e^{-i\omega t_p} + \hat{r}_{ps} e^{-i\omega t_{ps}}\right)$$

$$= \frac{r_0}{z_0}\left(1 - \hat{z}_p e^{-i\omega t_p} - \hat{z}_p \hat{r}_p e^{-2i\omega t_p} - \hat{z}_p \hat{r}_{ps} e^{-i\omega\left(t_p + t_{ps}\right)} + \hat{r}_p e^{-i\omega t_p} + \hat{r}_{ps} e^{-i\omega t_{ps}}\right)$$

neglecting higher order terms

$$= \frac{r_0}{z_0}\left(1 - \hat{z}_p e^{-i\omega t_p} + \hat{r}_p e^{-i\omega t_p} + \hat{r}_{ps} e^{-i\omega t_{ps}}\right)$$

plane wave means $\hat{z}_\mathrm{p} = \hat{\mathrm{r}}_\mathrm{p}$

$$\therefore \mathrm{R}(\omega) = \frac{r_0}{z_0} + r_{ps} e^{-i\omega t_{ps}}$$

P-wave

PS-wave

What factors influence r_0/z_0?

Isolating Mode Conversions

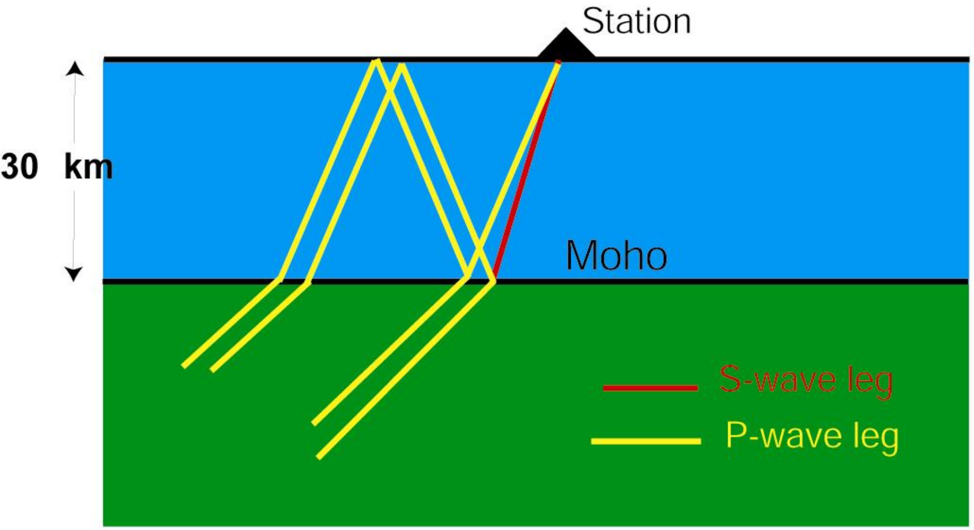

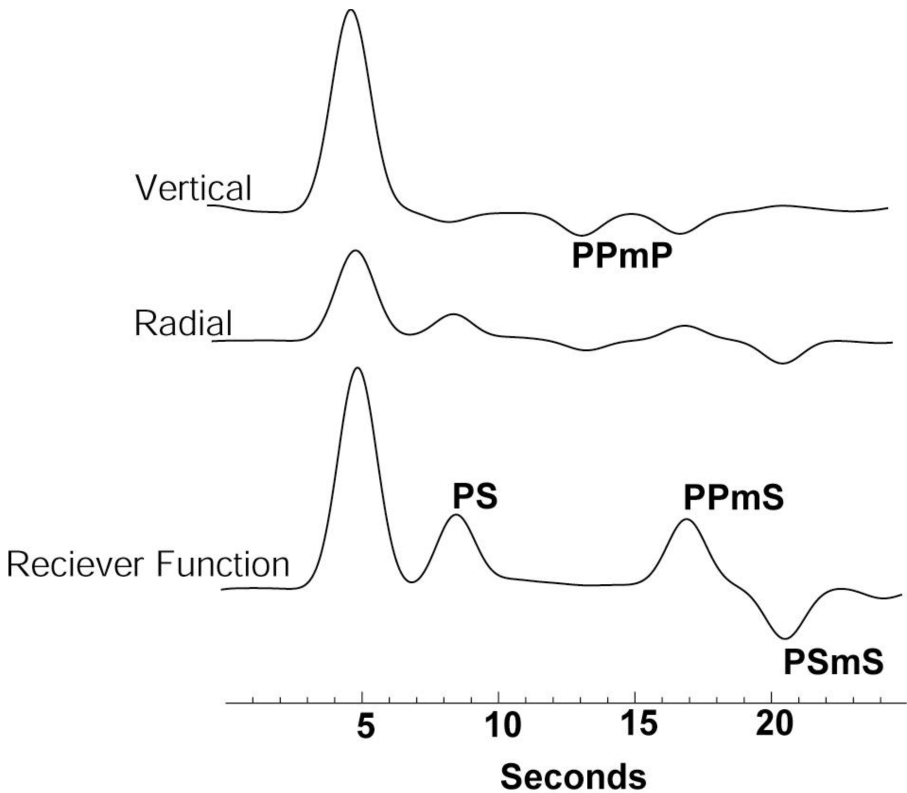

Methods of Deconvoltuion

- Spectral Division: water level technique

  (Burdick and Langston, 1978)
- Stacked Time Domain Deconvolution

  (Baker et al., 1996)
- Individual Iterative Time Domain Deconvolution

  (Liggoria and Ammon, 1999)

WATER-LEVEL DECONVOLUTION

•> water-level deconvolution introduced by Clayton & Wiggins

$$R(t) = \mathcal{F}^{-1}\left\{\frac{P^*(\omega)S(\omega)}{\max\left(P^*(\omega)P(\omega), cP^*_{\max}P_{\max}\right)}\right\}$$

•> for small *c* approaches deconvolution, large c approaches scaled cross-correlation

•> similar to damped least squares solution

$$R(t) = \mathcal{F}^{-1}\left\{\frac{P^*(\omega)S(\omega)}{P^*(\omega)P(\omega) + \delta}\right\}$$

Time Domain CONVOLUTIONAL MODEL

$$u_{in}(\mathbf{x},t) = S(t) \otimes G_{in}(\mathbf{x},t;\mathbf{p}_\perp)$$

$u_{in}(\mathbf{x},t)$

- observed displacement seismogram

$S(t)$

- effective source (includes source-side scattering)

$G_{in}(\mathbf{x},t;\mathbf{p}_\perp)$

- Green's function (receiver side response to an impulsive plane wave with horizontal slowness $\mathbf{p}_\perp$)

PS-phase Move-out:

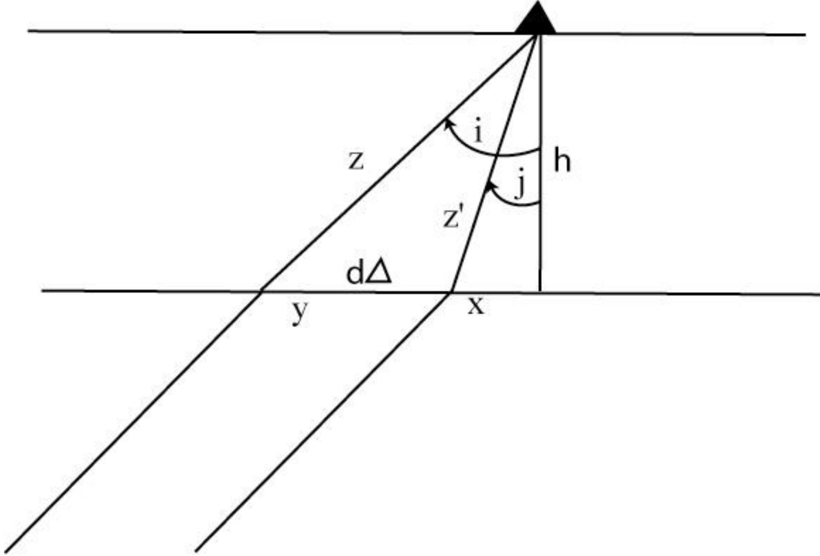

$$t_{PS-P} = t_{PS} - t_P = \frac{x}{V_s} - \frac{y}{V_p} - dT = \frac{h}{V_s \cos j} - \frac{h}{V_p \cos i} - dT$$

using

$$\sin i = V_p p, \sin j = V_s p \quad \therefore \cos i = \sqrt{1 - p^2 V_p{}^2}, \cos j = \sqrt{1 - p^2 V_S{}^2},$$

$$\text{then } t_{PS-P} = \frac{h\sqrt{1 - p^2 V_s{}^2}}{V_s} - \frac{h\sqrt{1 - p^2 V_p{}^2}}{V_p} - dT$$

$$= \frac{h\left(V_p \sqrt{1 - p^2 V_s{}^2} - V_s \sqrt{1 - p^2 V_p{}^2}\right)}{V_s V_p} - p d\Delta$$

Crustal Multiples:

$$t_{PPS} = h\left[\sqrt{V_s^{-2} - p^2} + \sqrt{V_p^{-2} - p^2}\right]$$

$$t_{PSS} = t_{PPS} + 2h\left[\sqrt{V_s^{-2} - p^2}\right]$$

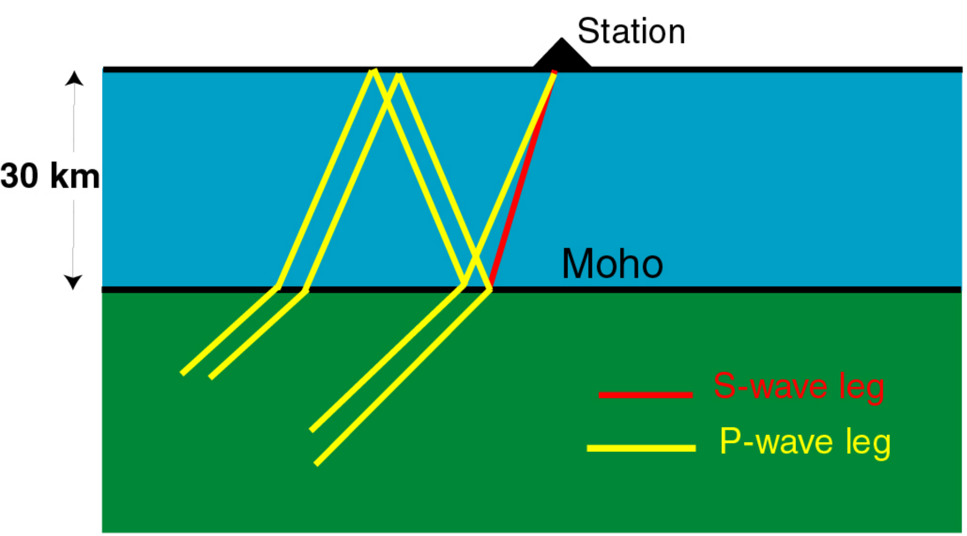

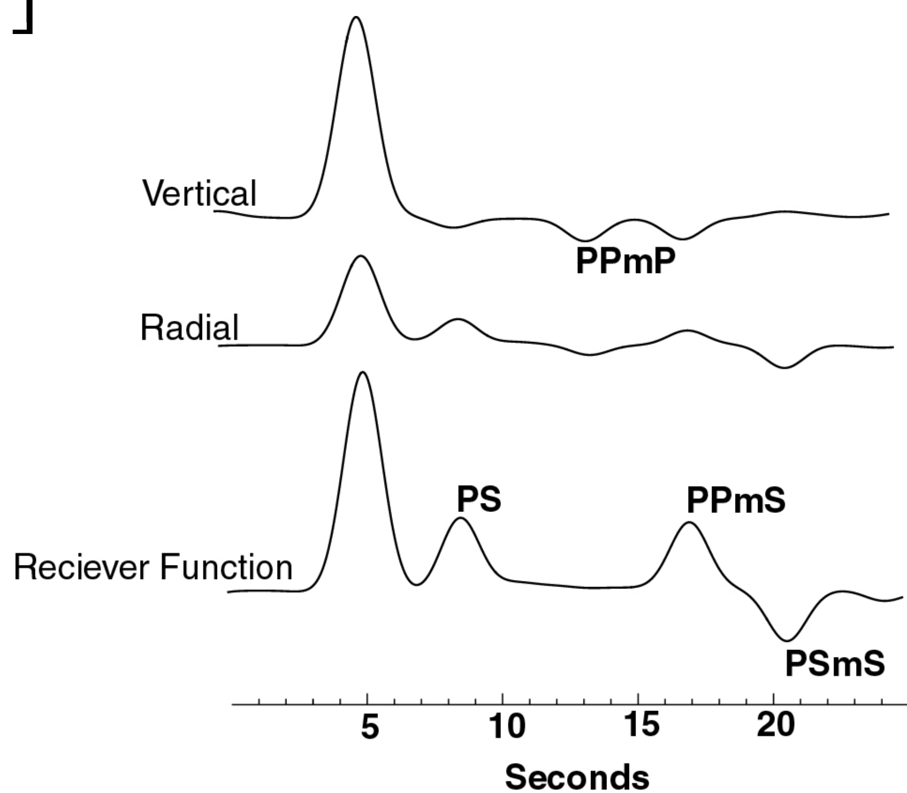

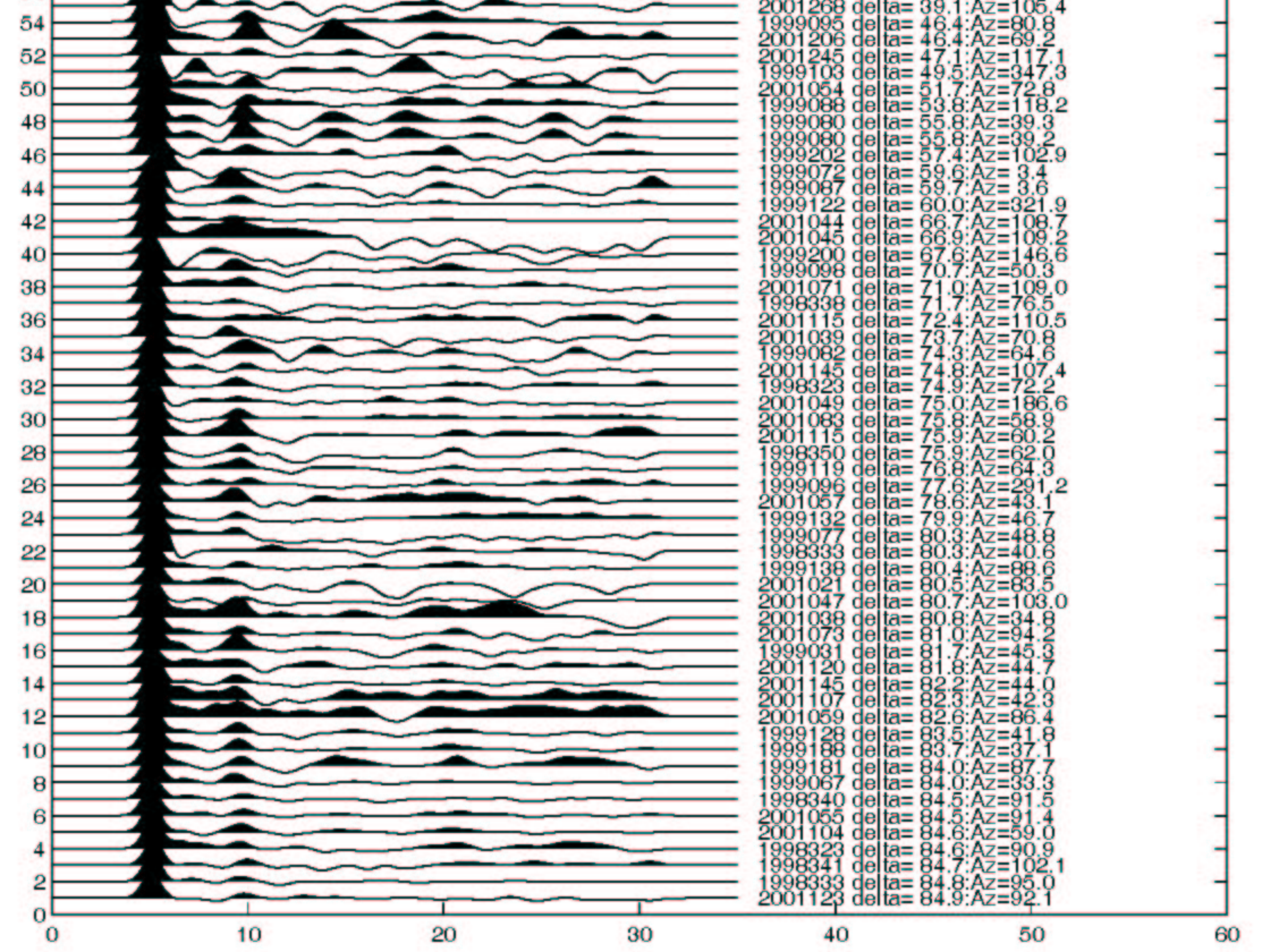
2001268 delta= 39.1:Az=105.4
1999095 delta= 46.4:Az=80.8
2001206 delta= 46.4:Az=69.2
2001245 delta= 47.1:Az=117.1
1999103 delta= 49.5:Az=347.3
2001054 delta= 51.7:Az=72.8
1999088 delta= 53.8:Az=118.2
1999080 delta= 55.8:Az=39.3
1999080 delta= 55.8:Az=39.2
1999202 delta= 57.4:Az=102.9
1999072 delta= 59.6:Az= 3.4
1999087 delta= 59.7:Az= 3.6
1999122 delta= 60.0:Az=321.9
2001044 delta= 66.7:Az=108.7
2001045 delta= 66.9:Az=109.2
1999200 delta= 67.6:Az=146.6
1999098 delta= 70.7:Az=50.3
2001071 delta= 71.0:Az=109.0
1998338 delta= 71.7:Az=76.5
2001115 delta= 72.4:Az=110.5
2001039 delta= 73.7:Az=70.8
1999082 delta= 74.3:Az=64.6
2001145 delta= 74.8:Az=107.4
1998323 delta= 74.9:Az=72.2
2001049 delta= 75.0:Az=186.6
2001083 delta= 75.8:Az=58.9
2001115 delta= 75.9:Az=60.2
1998350 delta= 75.9:Az=62.0
1999119 delta= 76.8:Az=64.3
1999096 delta= 77.6:Az=291.2
2001057 delta= 78.6:Az=43.1
1999132 delta= 79.9:Az=46.7
1999077 delta= 80.3:Az=48.8
1998333 delta= 80.3:Az=40.6
1999138 delta= 80.4:Az=88.6
2001021 delta= 80.5:Az=83.5
2001047 delta= 80.7:Az=103.0
2001038 delta= 80.8:Az=34.8
2001073 delta= 81.0:Az=94.2
1999031 delta= 81.7:Az=45.3
2001120 delta= 81.8:Az=44.7
2001145 delta= 82.2:Az=44.0
2001107 delta= 82.3:Az=42.3
2001059 delta= 82.6:Az=86.4
1999128 delta= 83.5:Az=41.8
1999188 delta= 83.7:Az=37.1
1999181 delta= 84.0:Az=87.7
1999067 delta= 84.0:Az=33.3
1998340 delta= 84.5:Az=91.5
2001055 delta= 84.5:Az=91.4
2001104 delta= 84.6:Az=59.0
1998323 delta= 84.6:Az=90.9
1998341 delta= 84.7:Az=102.1
1998333 delta= 84.8:Az=95.0
2001123 delta= 84.9:Az=92.1
0
10
20
30
40
50
60

SCATTERING GEOMETRY

•> consider plane P wave incident from below

•> receiver side scattering includes forward and back scattering, P and S

•> legs ending in P and S isolated through modal decomposition

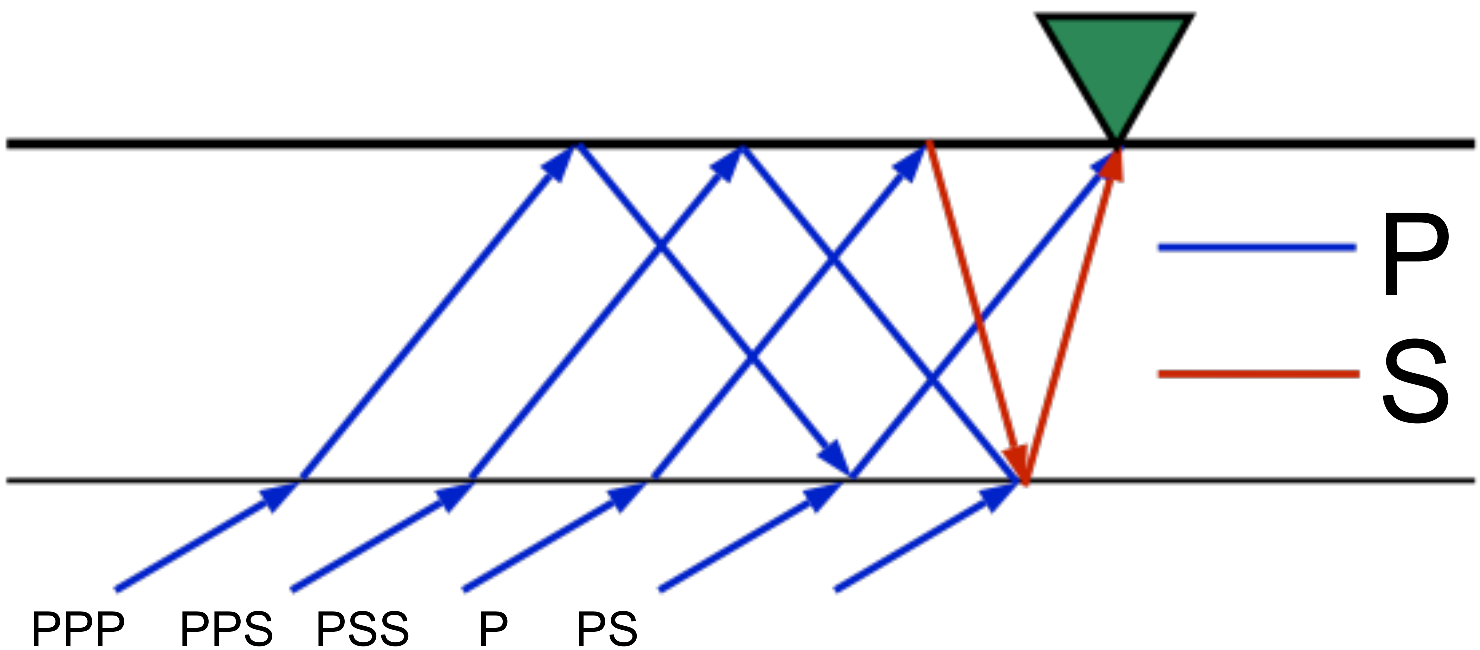

Slant Stacking

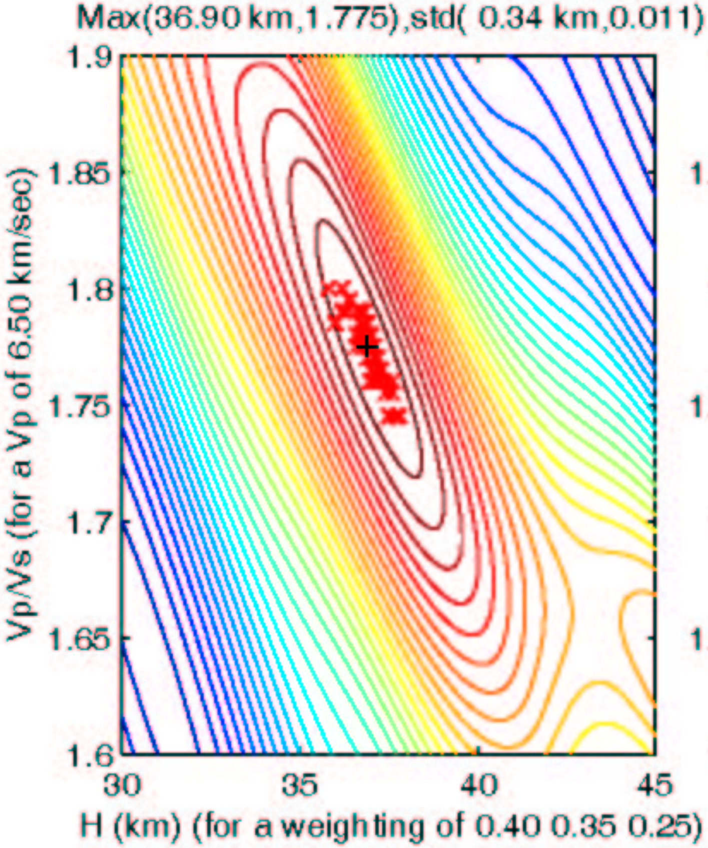

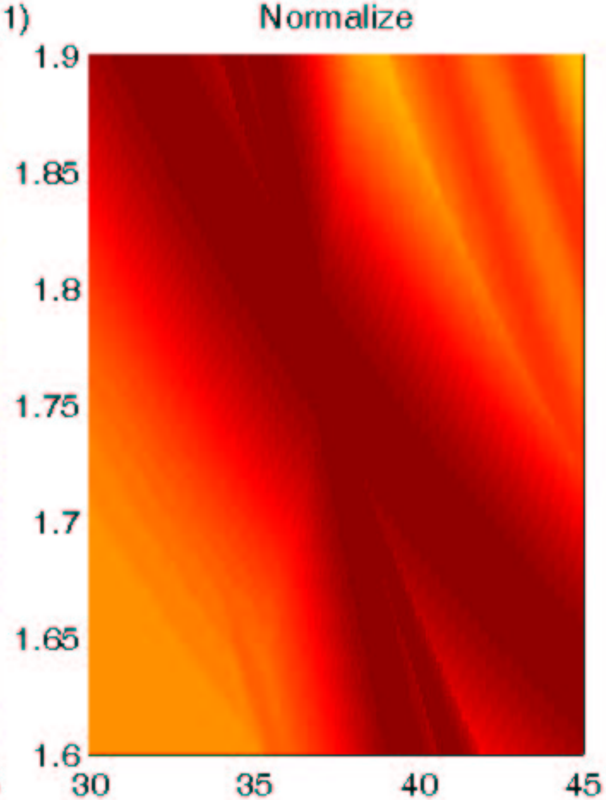

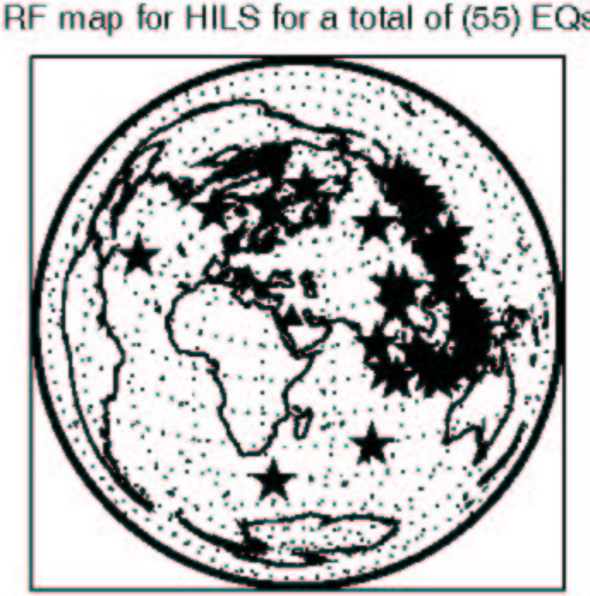

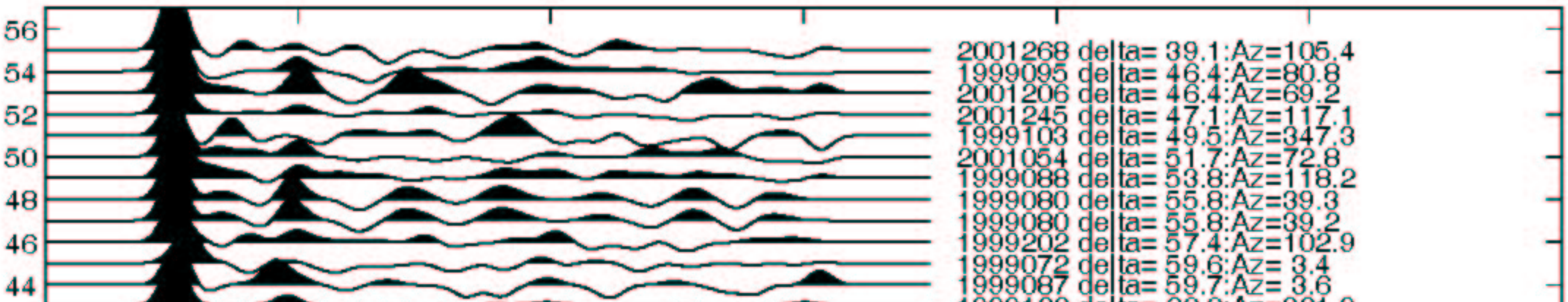

Synthetic Receiver Functions:

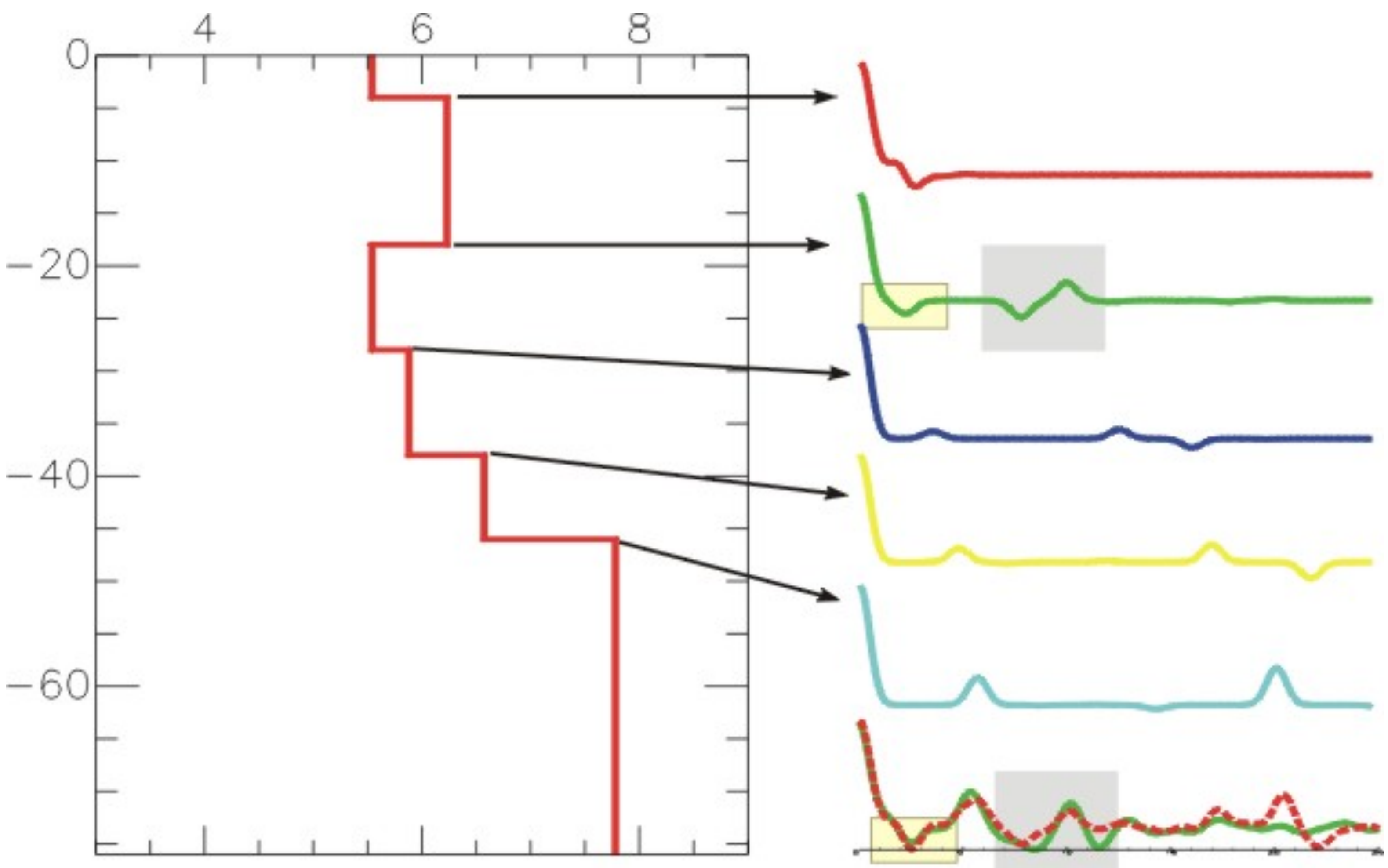

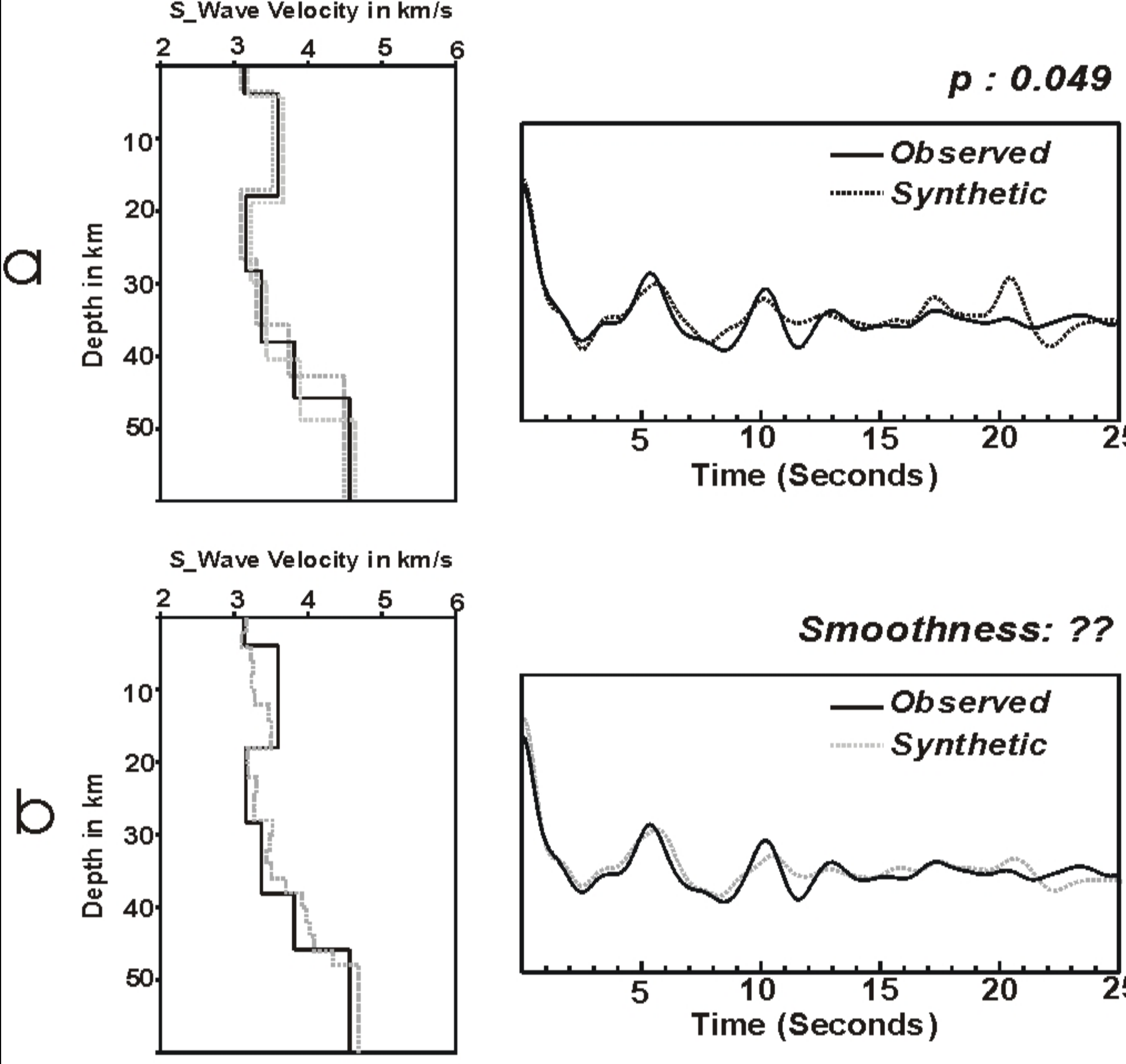

S_Wave Velocity in km/s
2
3
4
5
6
Depth in km
10
20
30
40
50
a
p : 0.049
Observed
Synthetic
5
10
15
20
25
Time (Seconds)
S_Wave Velocity in km/s
2
3
4
5
6
Depth in km
10
20
30
40
50
b
Smoothness: ??
Observed
Synthetic
5
10
15
20
25
Time (Seconds)

LEAST-SQUARES INVERSION

•> receiver function inversion cast in standard inverse theory framework

•> less expensive than MC/DS methods and makes less stringent demands on data than inverse scattering methods

•> data insufficiency compensated for by regularization (e.g. damping)

•> like MC/DS methods LS involves model matching so there is no formal requirement that data are delivered as Green's functions (e.g. receiver function is adequate); only a forward modelling engine is strictly required

Receiver Functions

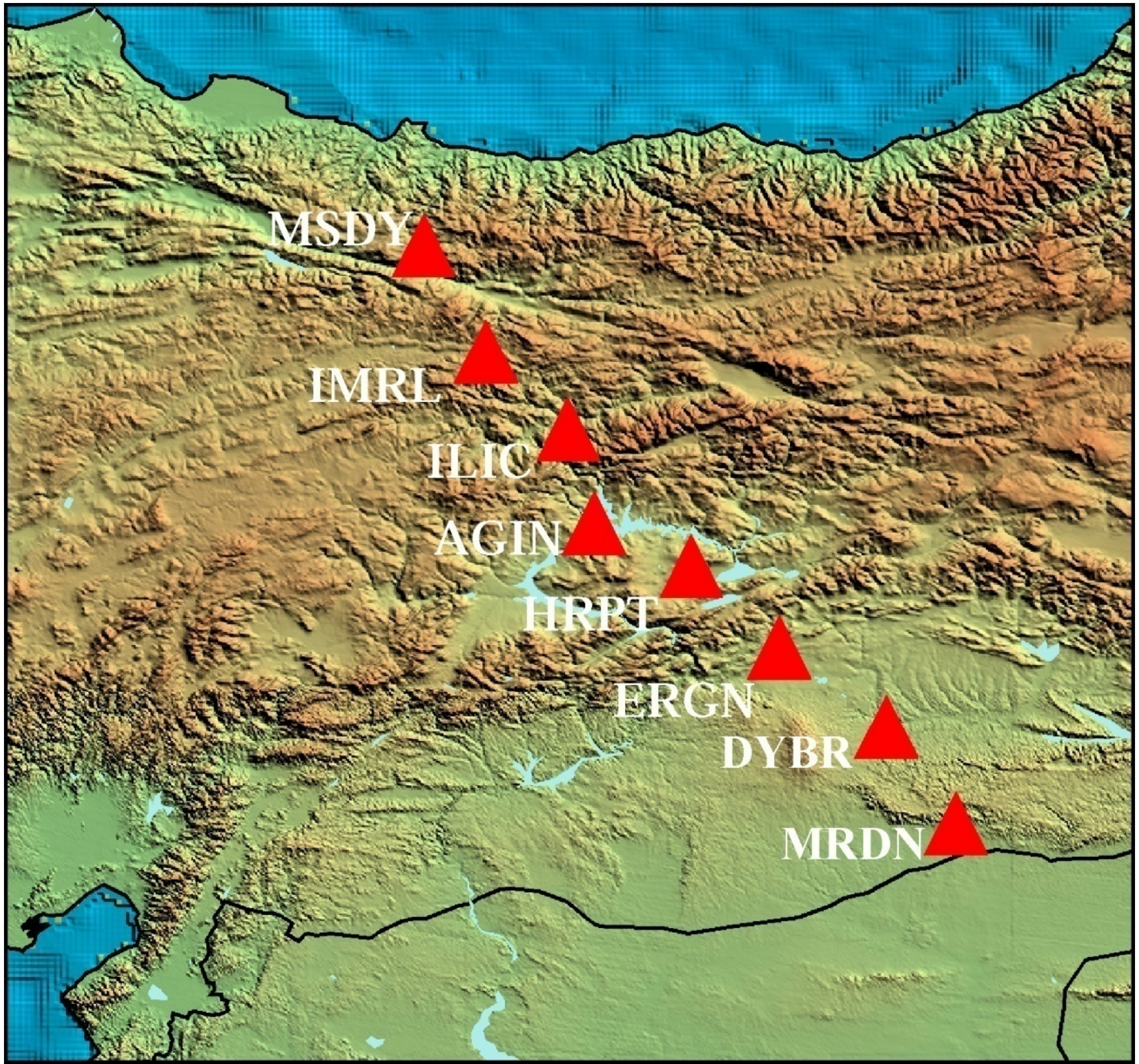

WESTERN PR

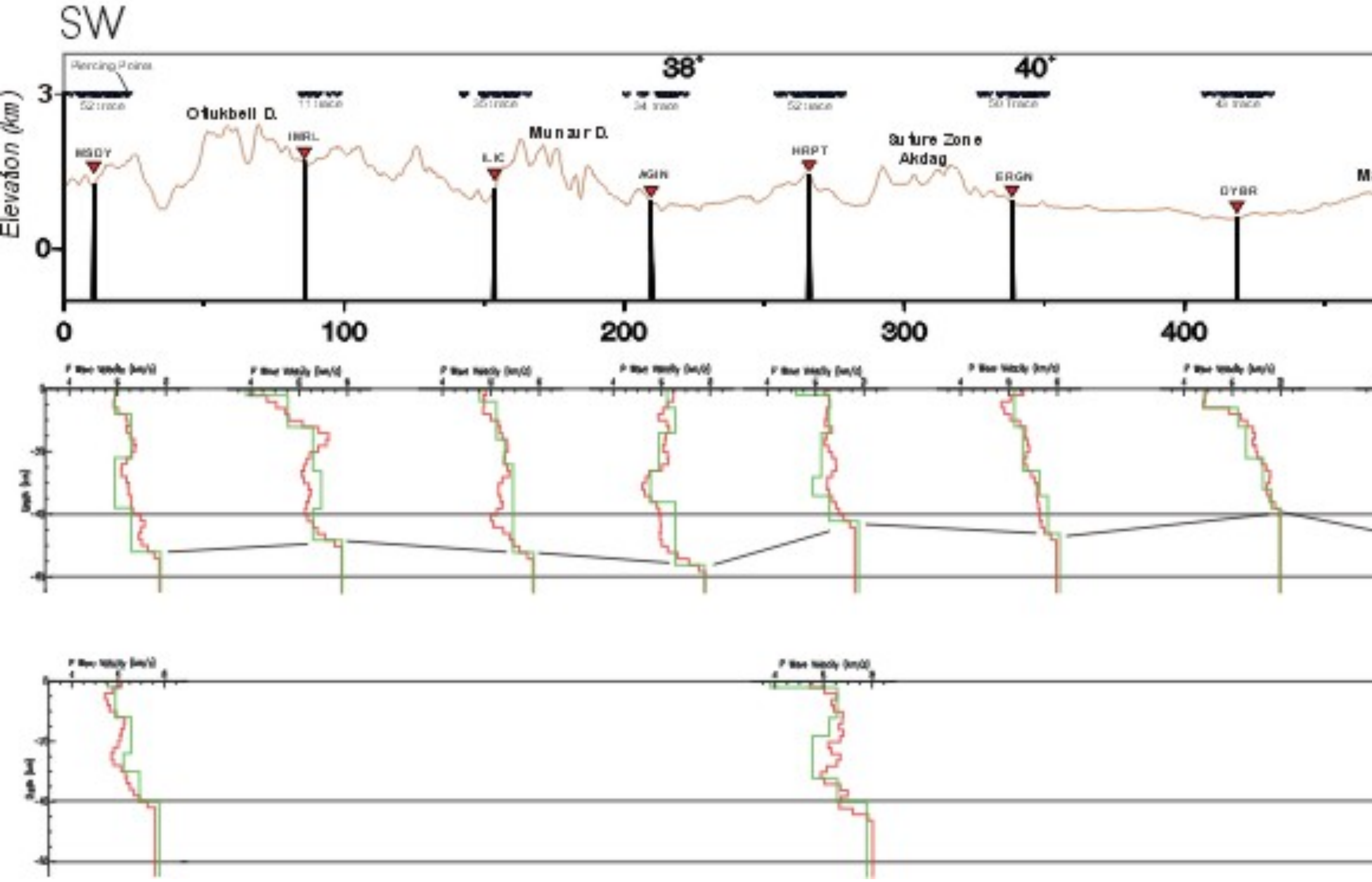

SW
Elevation (km)
3
0
Piercing Points
38°
40°
Munzur D.
Suture Zone
Akdag
INRL
ILIC
AGIN
HRPT
ERGN
DYBR
0
100
200
300
400

Receiver Function Footprints

15 km Interface

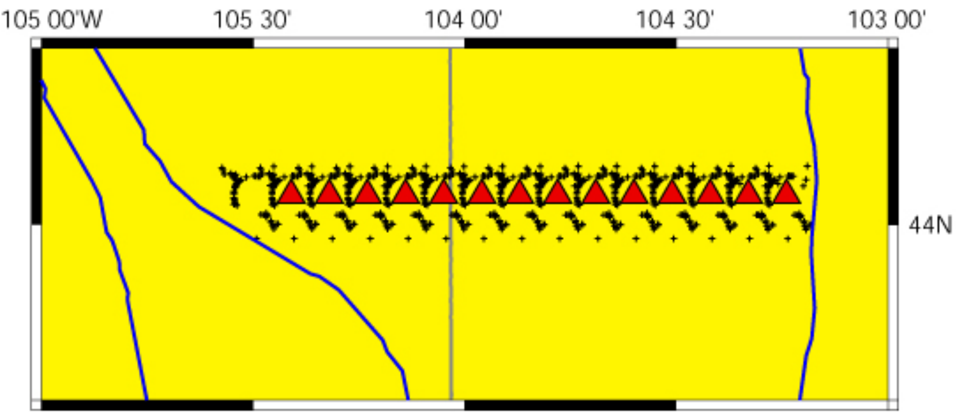

40 km Interface

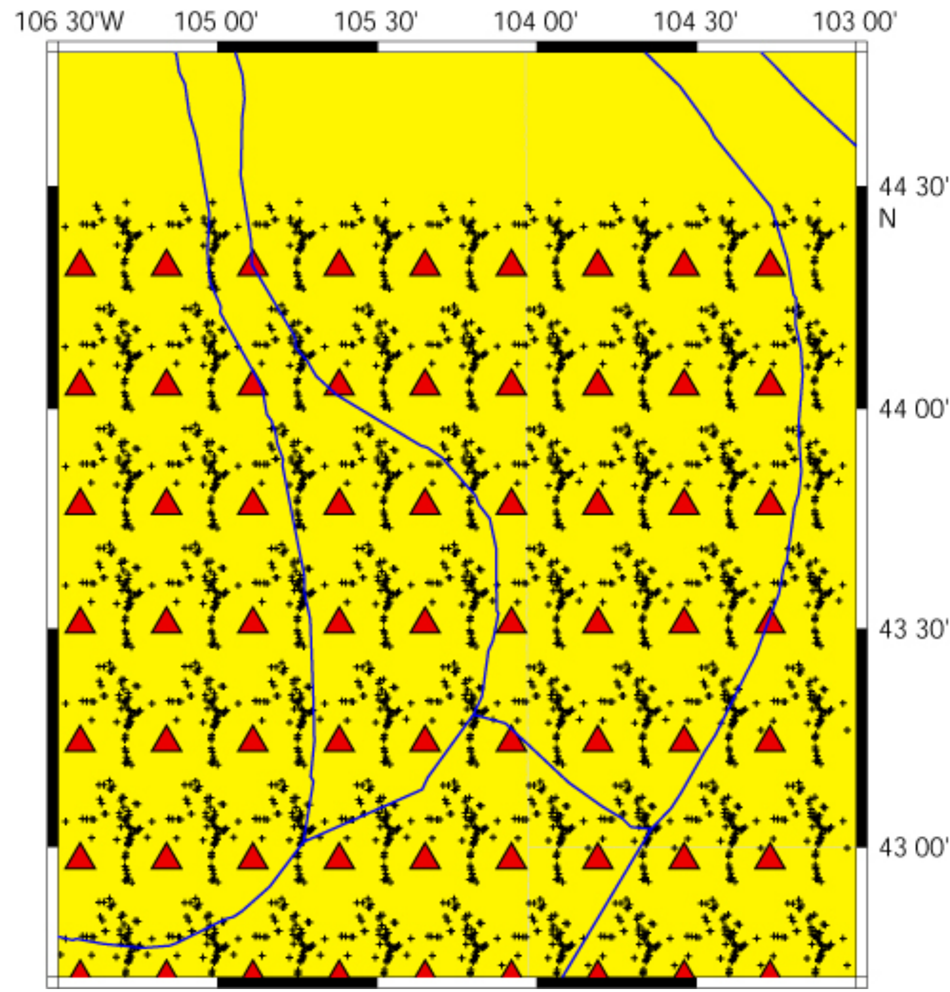

Migrating Receiver Functions

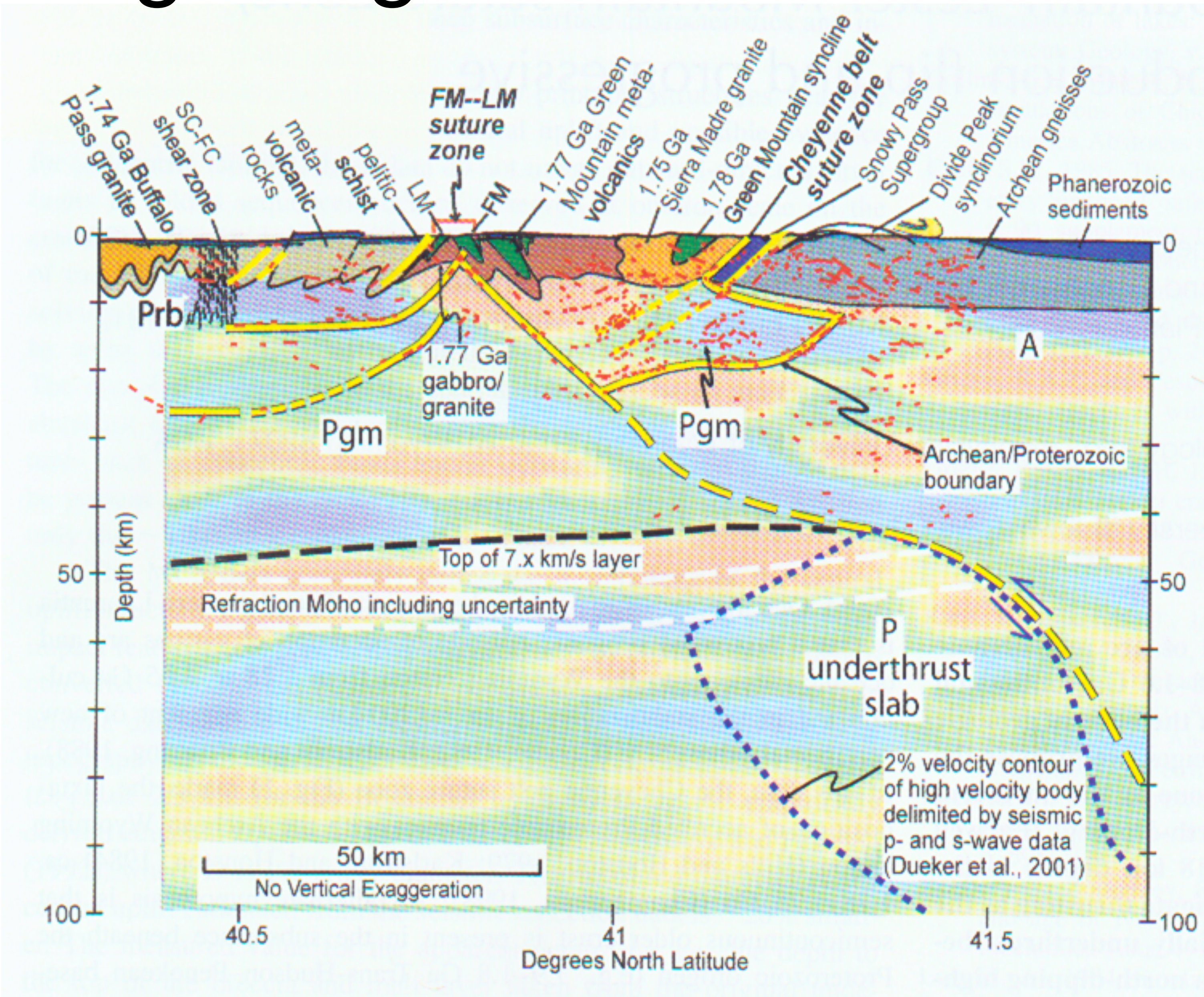

ASCENT P-wave Receiver Functions

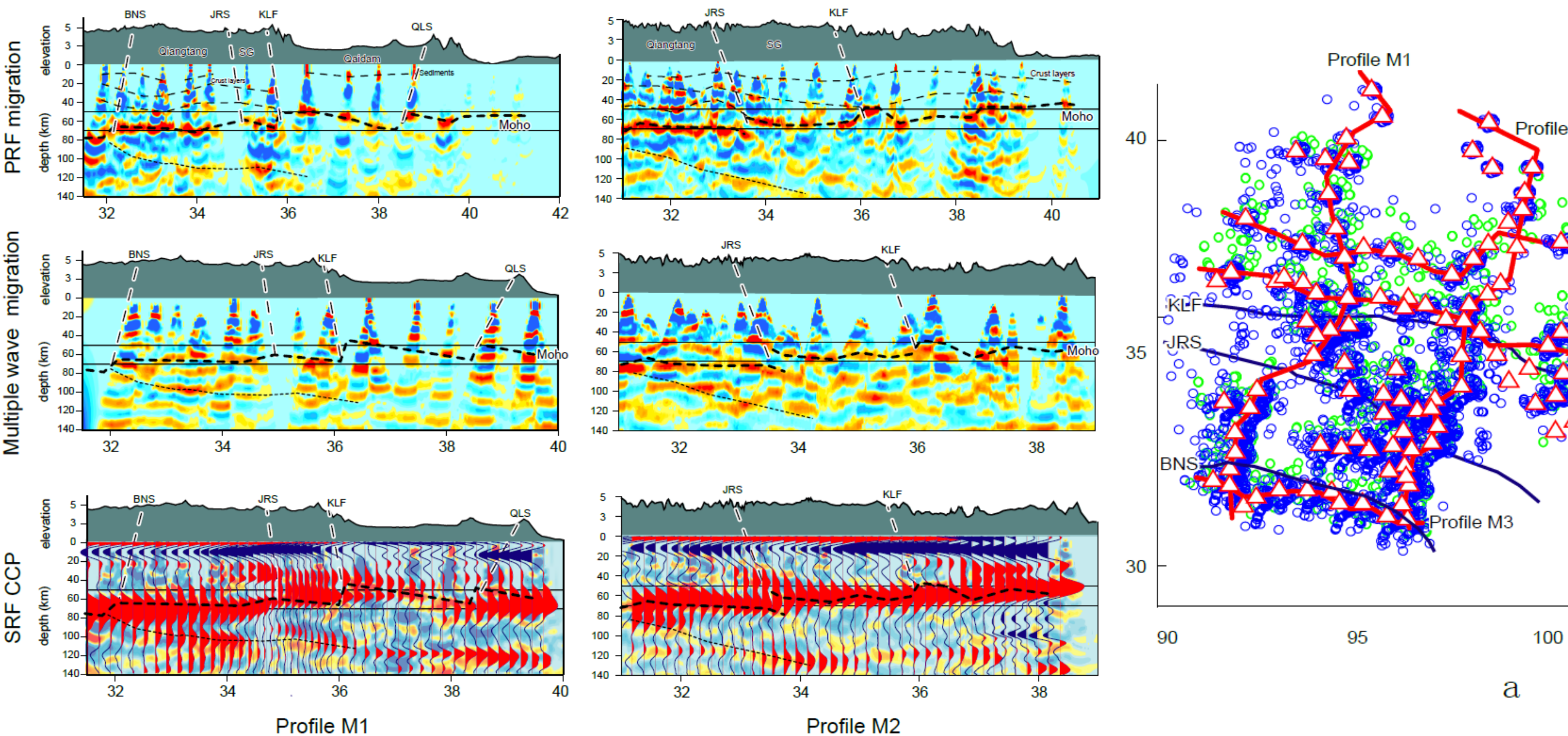

S wave Receiver Functions

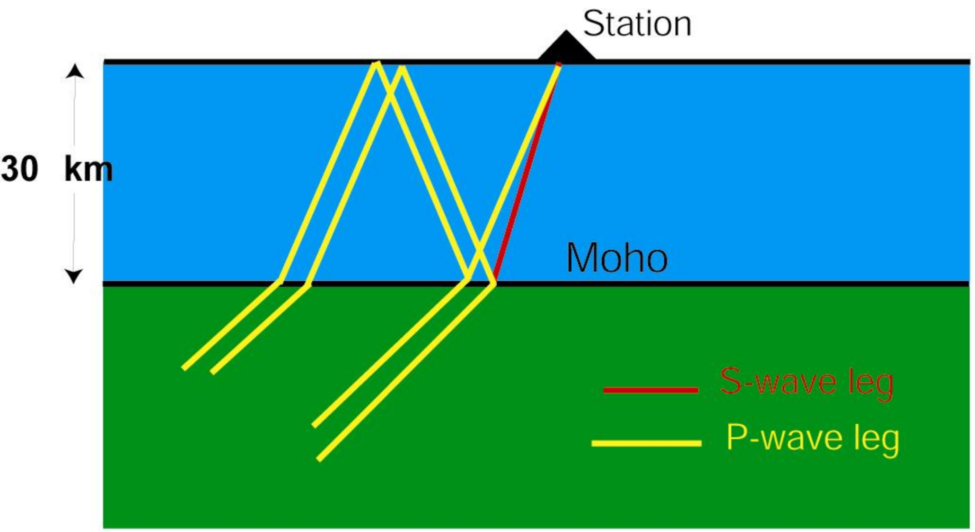

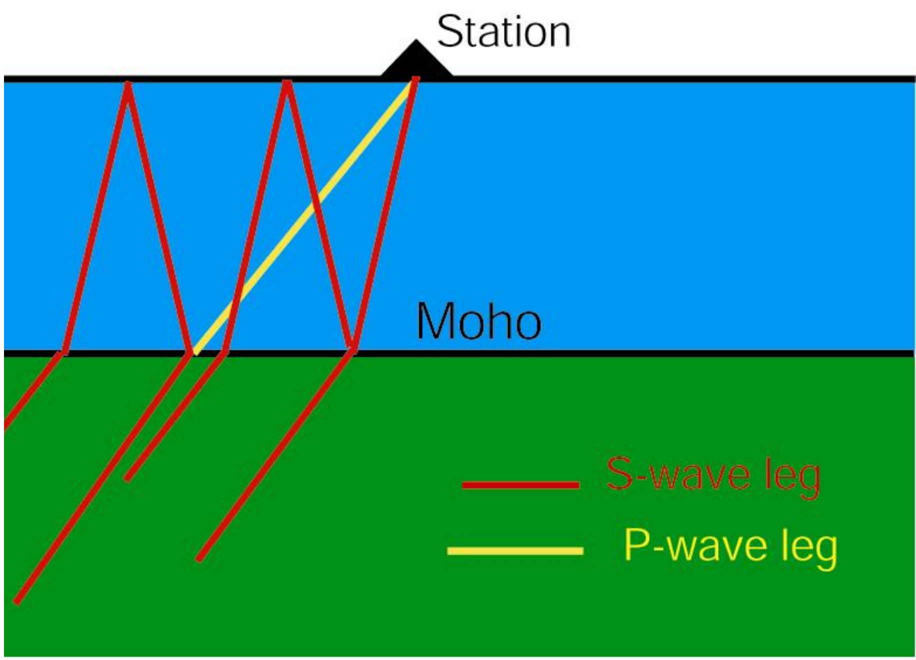

S Receiver Functions

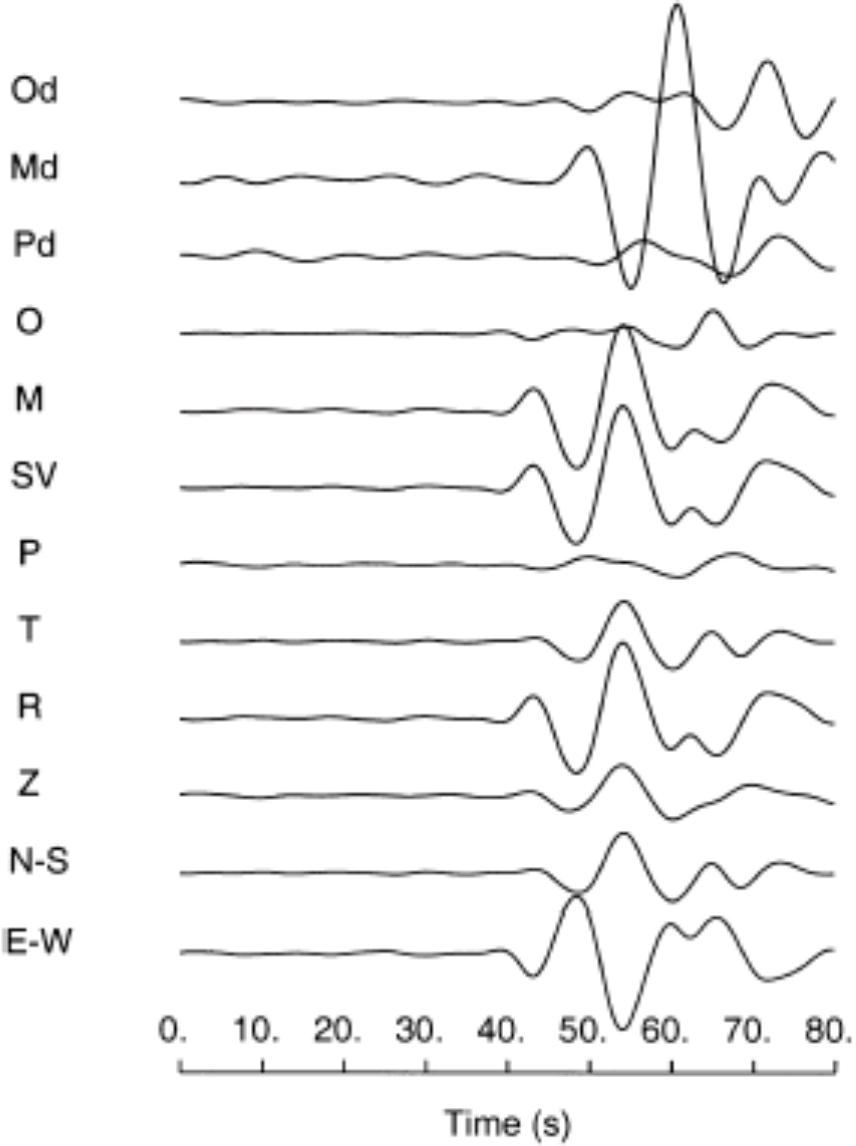

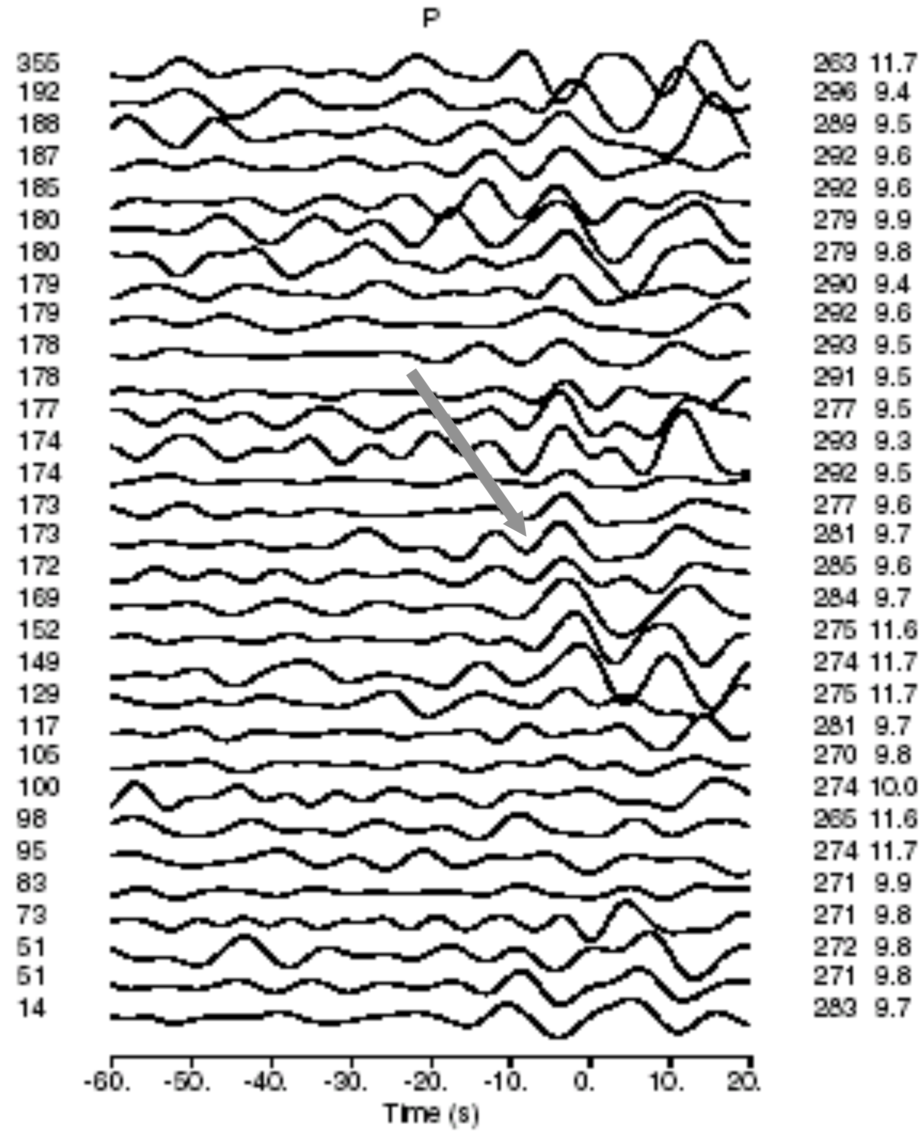

From Farra and Vinnik, 2000

Comparisons with P Receiver Functions

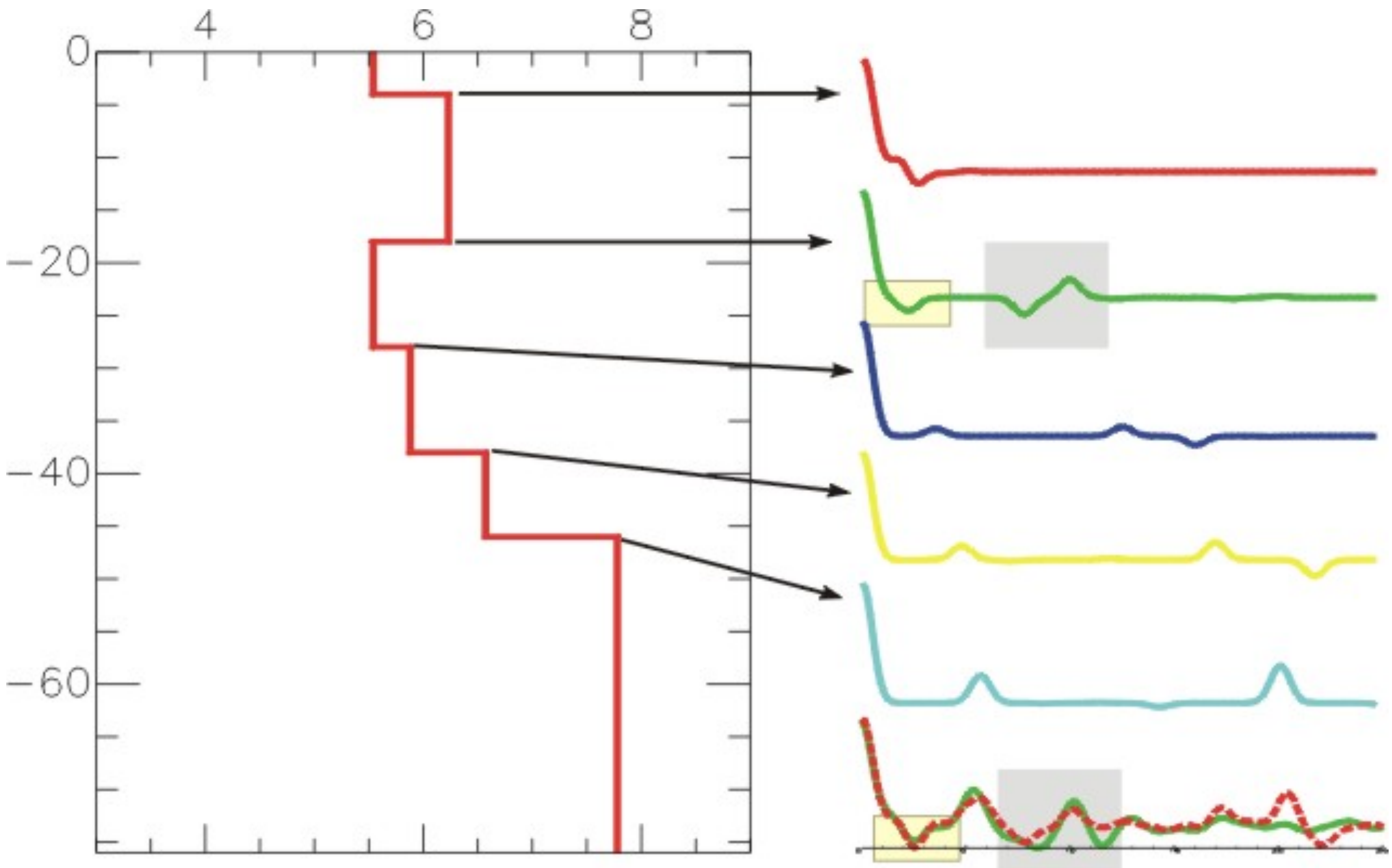

Migrated S-wave Receiver Functions

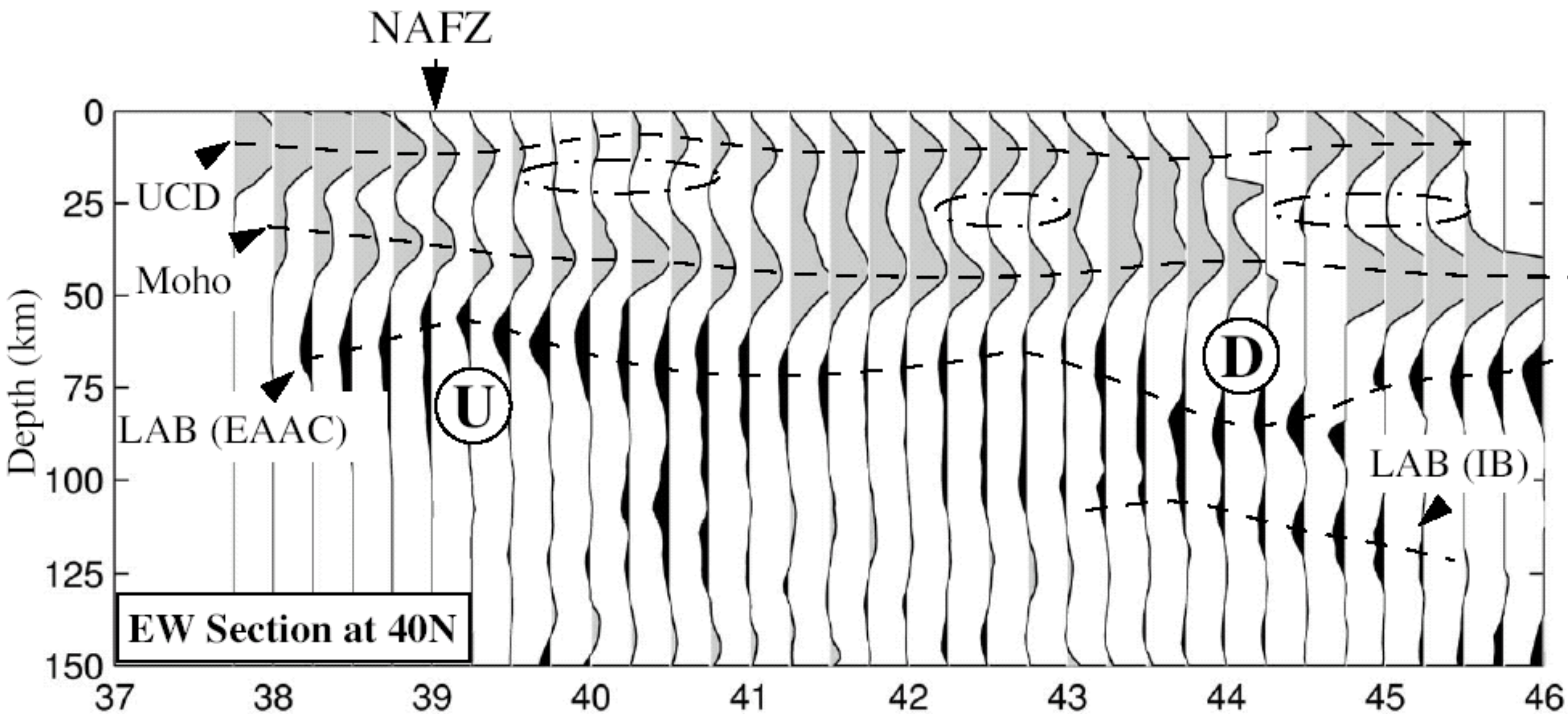

Angus et al., 2005

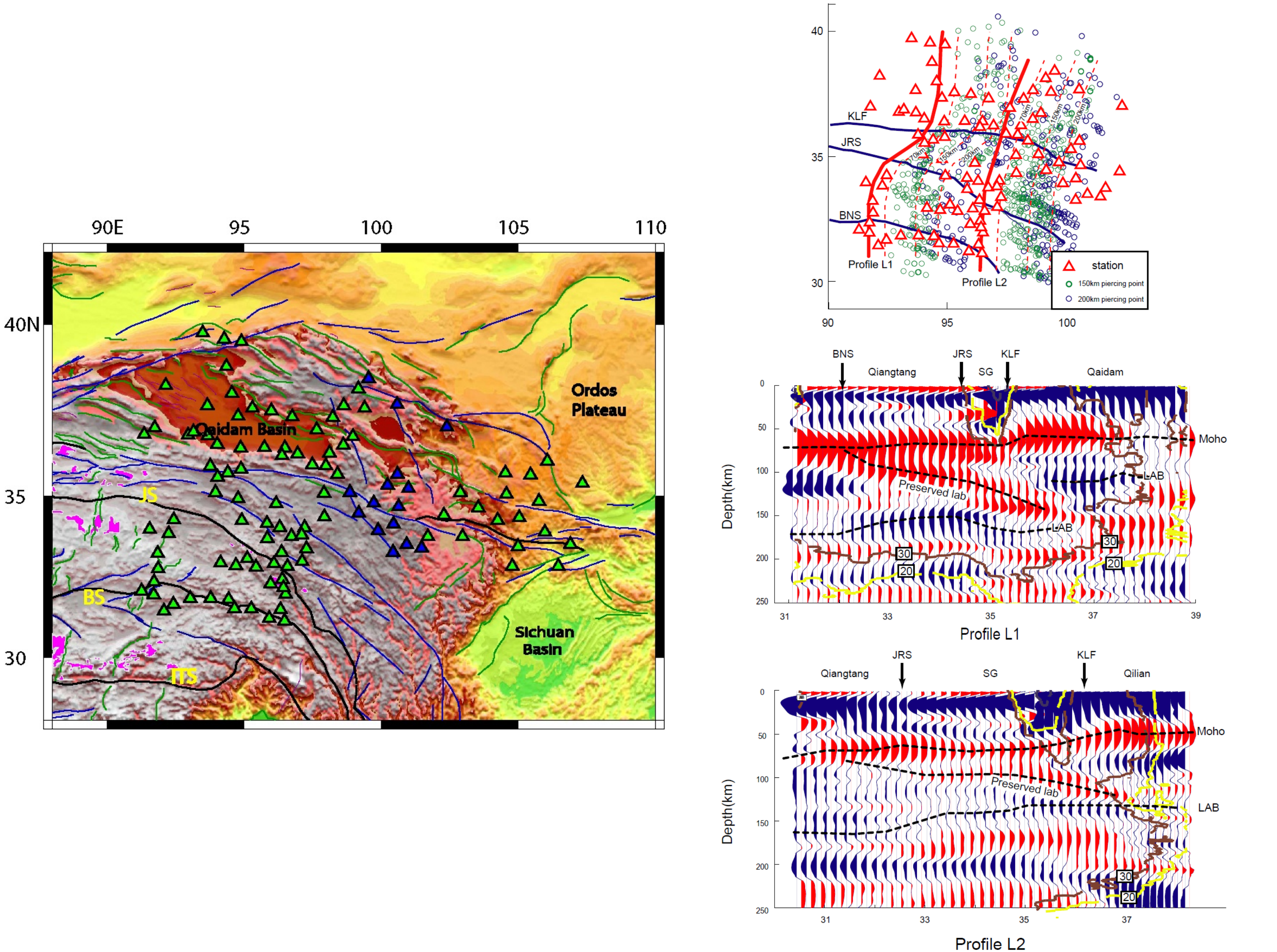

90E
95
100
105
110
40N
35
30
Qaidam Basin
Ordos Plateau
Sichuan Basin
JS
BS
TTS
KLF
JRS
BNS
Profile L1
Profile L2
station
150km piercing point
200km piercing point
70km
150km
200km
BNS
Qiangtang
JRS
SG
KLF
Qaidam
Moho
LAB
Preserved lab
30
20
Depth(km)
31
33
35
37
39
Profile L1
Qiangtang
JRS
SG
KLF
Qilian
Moho
Preserved lab
LAB
Depth(km)
Profile L2

For Next Time:
Mike Pasyanos:Surface Wave Dispersion

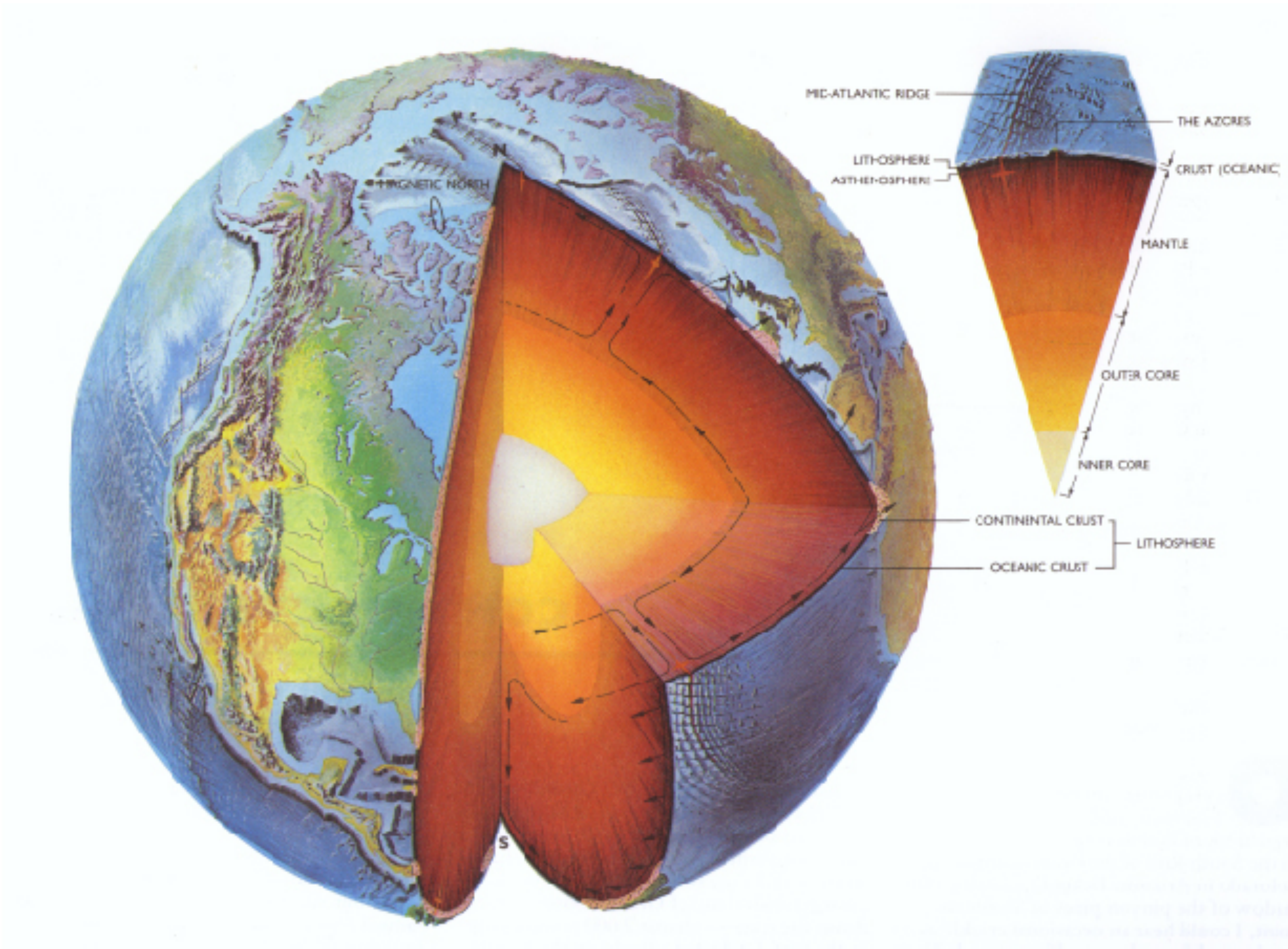

SIMULTANEOUS DECONVOLUTION

•> when large numbers of seismograms representing a single receiver/Green's function are available, perform simultaneous, least-squares deconvolution

$$R(t) = \mathcal{F}^{-1}\left\{\frac{\sum_i P_i^*(\omega)S_i(\omega)}{\sum_i P_i^*(\omega)P_i(\omega) + \delta}\right\}$$

•> advantageous due to fact that smaller sum of spectra in denominator reduce likelihood of spectral zeros allowing for smaller values of water level parameter δ to be used

•> Gurrola et al, 1995, GJI, 120, 537-543

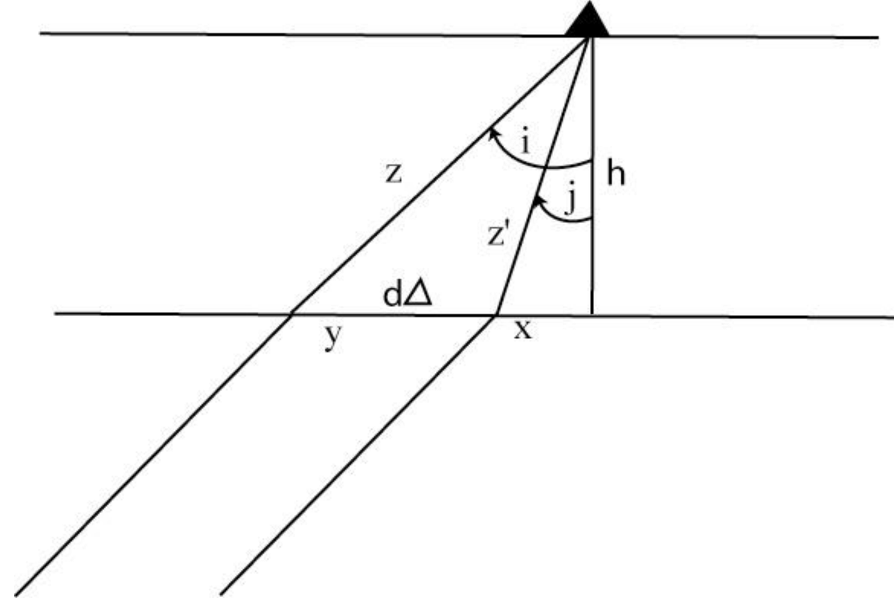

$$t_{PS-P} = \frac{h\left(V_p\sqrt{1-p^2V_s^{\,2}} - V_s\sqrt{1-p^2V_p^{\,2}}\right)}{V_sV_p\sqrt{1-p^2V_p^{\,2}}\sqrt{1-p^2V_s^{\,2}}} - d\Delta p$$

$$= \frac{h\left(V_p\sqrt{1-p^2V_s^{\,2}} - V_s\sqrt{1-p^2V_p^{\,2}}\right)}{V_sV_p\sqrt{1-p^2V_p^{\,2}}\sqrt{1-p^2V_s^{\,2}}} + p(y-x)$$

$$x = h\tan j = \frac{hV_sp}{\sqrt{1-p^2V_s^{\,2}}}, y = h\tan i = \frac{hV_pp}{\sqrt{1-p^2V_p^{\,2}}}$$

$$\therefore t_{PS-P} = \frac{h\left(V_p\sqrt{1-p^2V_s^{\,2}} - V_s\sqrt{1-p^2V_p^{\,2}}\right)}{V_sV_p\sqrt{1-p^2V_p^{\,2}}\sqrt{1-p^2V_s^{\,2}}} + hp^2\frac{V_p\sqrt{1-p^2V_s^{\,2}} - V_s\sqrt{1-p^2V_p^{\,2}}}{\sqrt{1-p^2V_s^{\,2}}\sqrt{1-p^2V_p^{\,2}}}$$

$$= h\left[\frac{\left(V_p\sqrt{1-p^2V_s^{\,2}} - V_s\sqrt{1-p^2V_p^{\,2}}\right) + p^2V_p^{\,2}V_s\sqrt{1-p^2V_s^{\,2}} - p^2V_s^{\,2}V_p\sqrt{1-p^2V_p^{\,2}}}{V_sV_p\sqrt{1-p^2V_s^{\,2}}\sqrt{1-p^2V_p^{\,2}}}\right]$$

$$= h\left[\frac{V_p\sqrt{1-p^2V_s^{\,2}}\left(1-p^2V_s^{\,2}\right) - V_s\sqrt{1-p^2V_p^{\,2}}\,(1-p^2V_p^{\,2})}{V_sV_p\sqrt{1-p^2V_s^{\,2}}\sqrt{1-p^2V_p^{\,2}}}\right] = h\left[\sqrt{V_s^{\,-2}-p^2} - \sqrt{V_p^{\,-2}-p^2}\right]$$

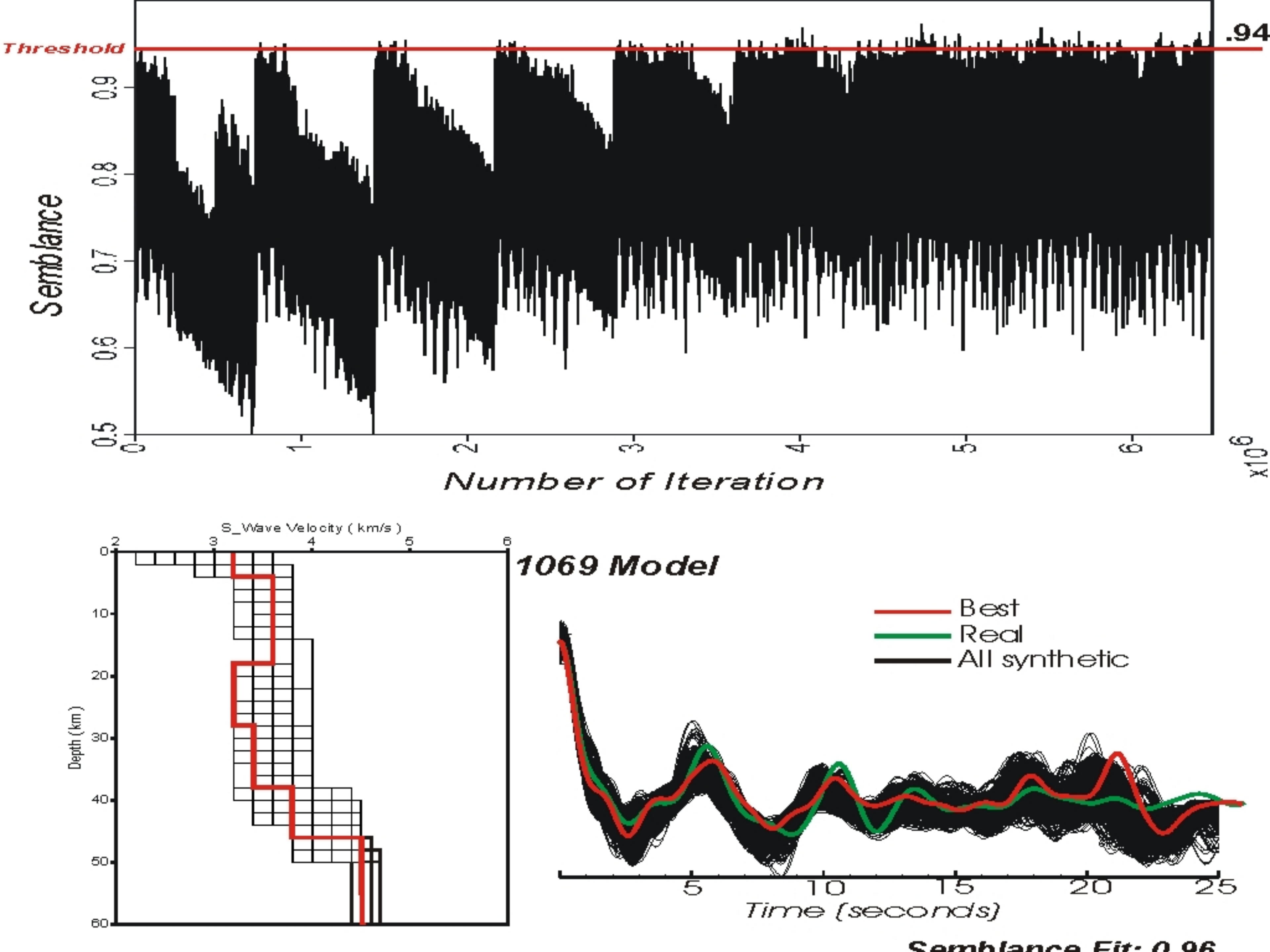

Threshold
.94
Semblance
0.5
0.6
0.7
0.8
0.9
0
1
2
3
4
5
6
x10^6
Number of Iteration
S_Wave Velocity (km/s)
2
3
4
5
6
0
10
20
30
40
50
60
Depth (km)
1069 Model
Best
Real
All synthetic
5
10
15
20
25
Time (seconds)
Semblance Fit: 0.96

Background: Geodynamic models of Tibetan plate

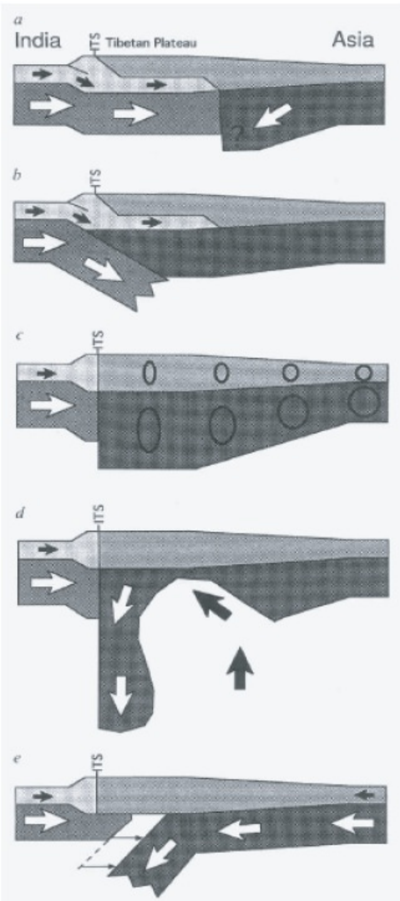

[*Willett* and *Beaumont*, 1994]

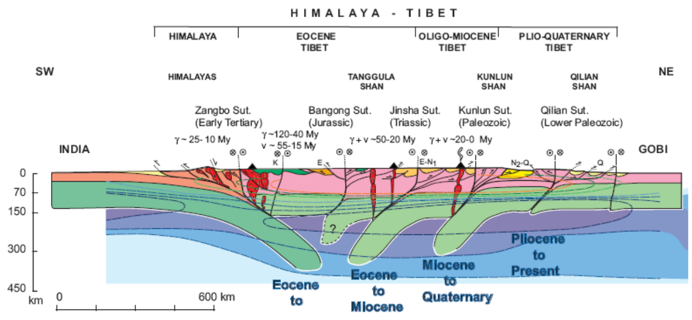

[*Tapponnier et al.*, 2001]

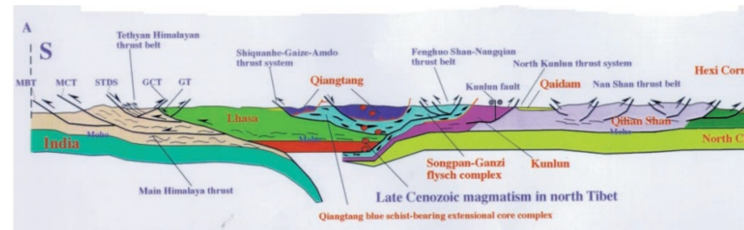

[*Yin and Harrison*, 2000]

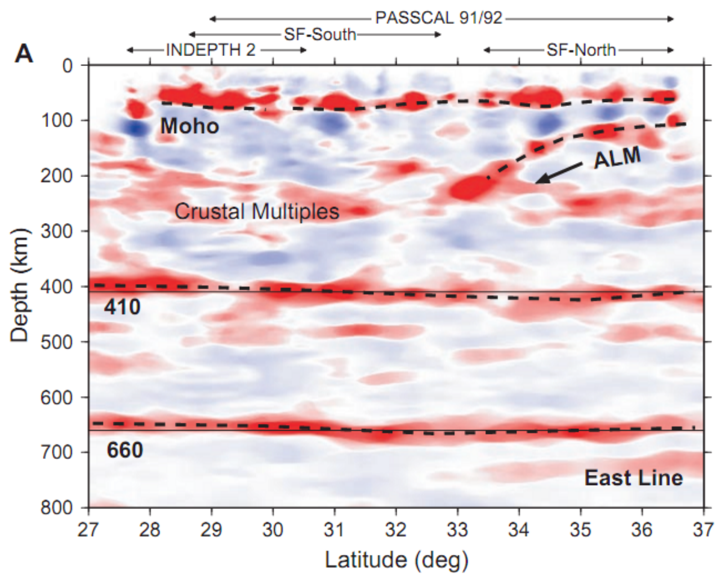

[Kind et al., 2002]

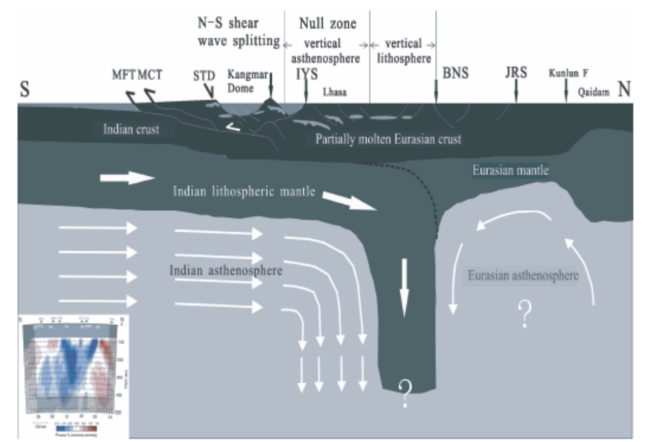

[*Fu et al.*, 2008]

Unknown deep structure

Mainly north-south profiles

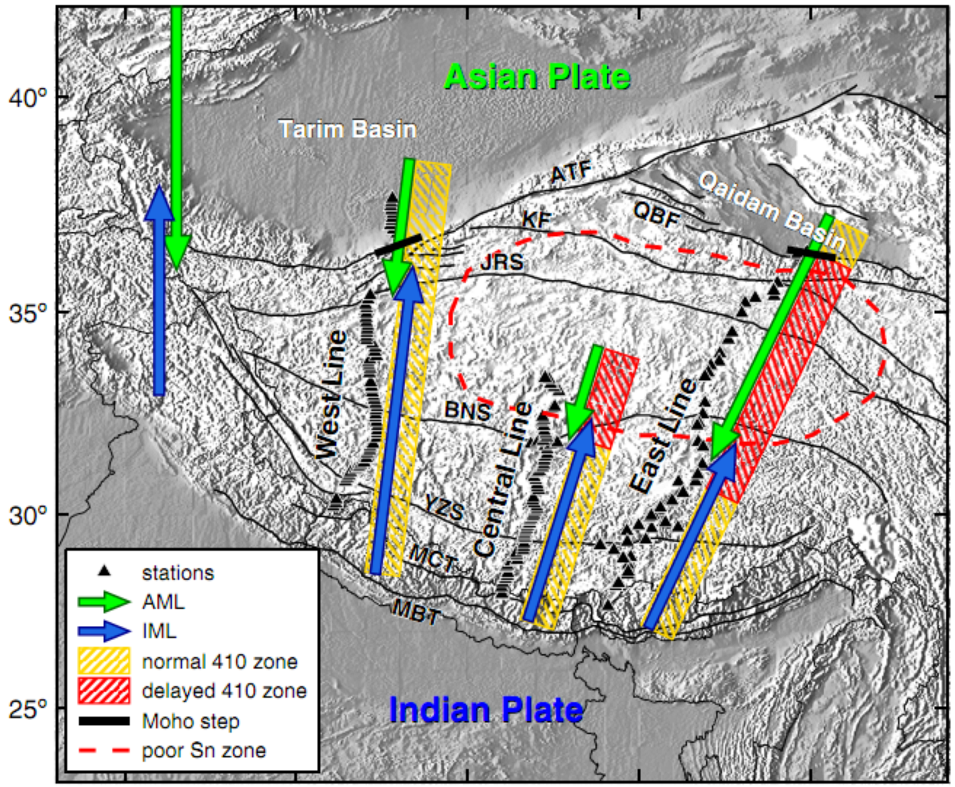

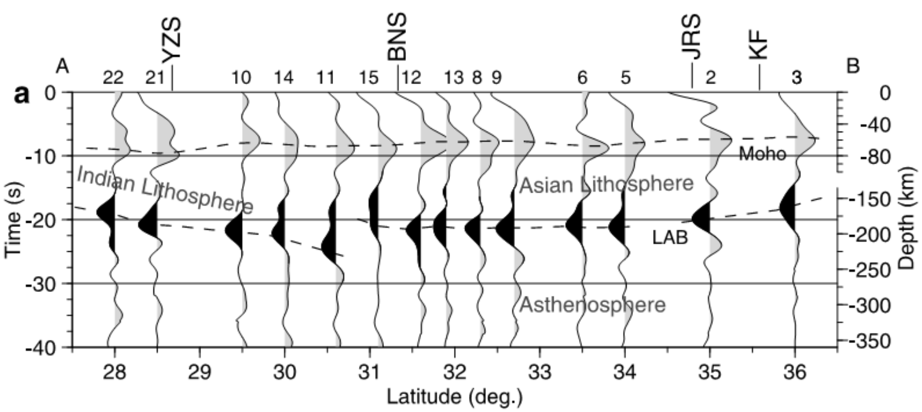

[Kumar et al.,

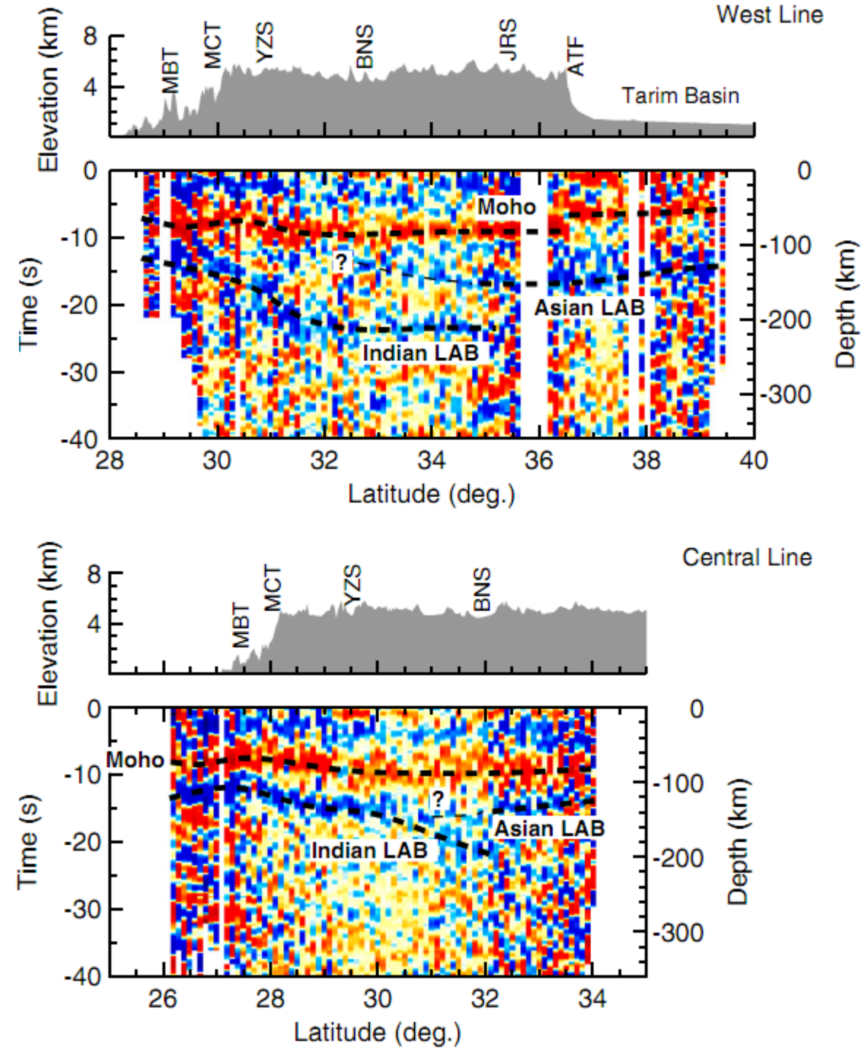

[Zhao et al., 2010]

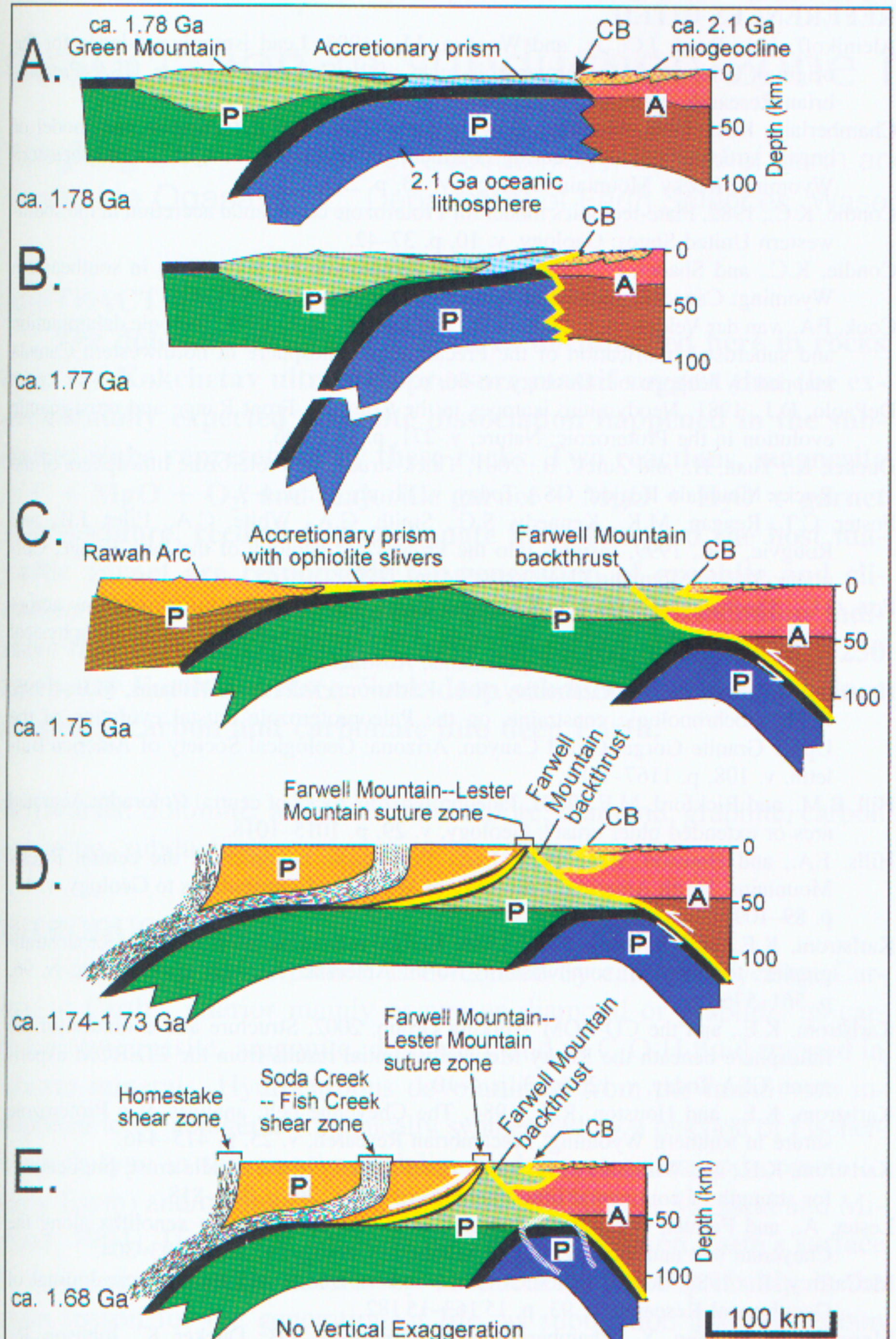
A.
ca. 1.78 Ga
Green Mountain
Accretionary prism
CB
ca. 2.1 Ga
miogeocline
0
50
100
Depth (km)
P
P
A
2.1 Ga oceanic
lithosphere
ca. 1.78 Ga
B.
CB
P
P
A
0
50
100
ca. 1.77 Ga
C.
Rawah Arc
Accretionary prism
with ophiolite slivers
Farwell Mountain
backthrust
CB
P
P
A
P
0
50
100
ca. 1.75 Ga
D.
Farwell Mountain--Lester
Mountain suture zone
Farwell
Mountain
backthrust
CB
P
P
A
P
0
50
100
ca. 1.74-1.73 Ga
E.
Homestake
shear zone
Soda Creek
-- Fish Creek
shear zone
Farwell Mountain--
Lester Mountain
suture zone
Farwell Mountain
backthrust
CB
P
P
A
P
0
50
100
Depth (km)
ca. 1.68 Ga
No Vertical Exaggeration
100 km

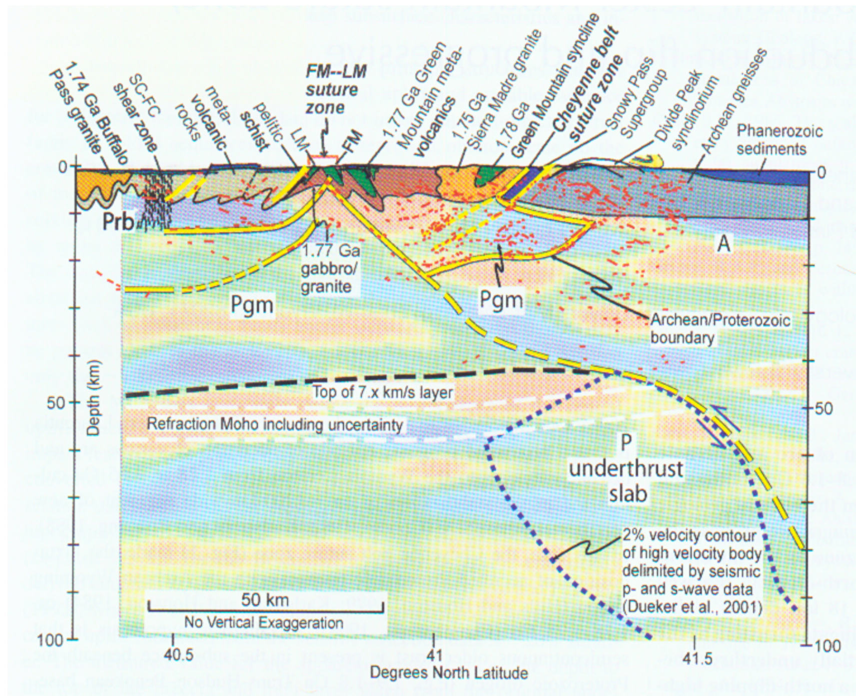
1.74 Ga Buffalo
Pass granite
SC-FC
shear zone
meta-
volcanic
rocks
pelitic
schist
LM
FM--LM
suture
zone
FM
1.77 Ga Green
Mountain meta-
volcanics
1.75 Ga
Sierra Madre granite
1.78 Ga
Green Mountain syncline
Cheyenne belt
suture zone
Snowy Pass
Supergroup
Divide Peak
synclinorium
Archean gneisses
Phanerozoic
sediments
Prb
1.77 Ga
gabbro/
granite
Pgm
Pgm
A
Archean/Proterozoic
boundary
Top of 7.x km/s layer
Refraction Moho including uncertainty
P
underthrust
slab
2% velocity contour
of high velocity body
delimited by seismic
p- and s-wave data
(Dueker et al., 2001)
50 km
No Vertical Exaggeration
Depth (km)
0
50
100
40.5
41
41.5
Degrees North Latitude

Migrated S-wave Receiver Functions

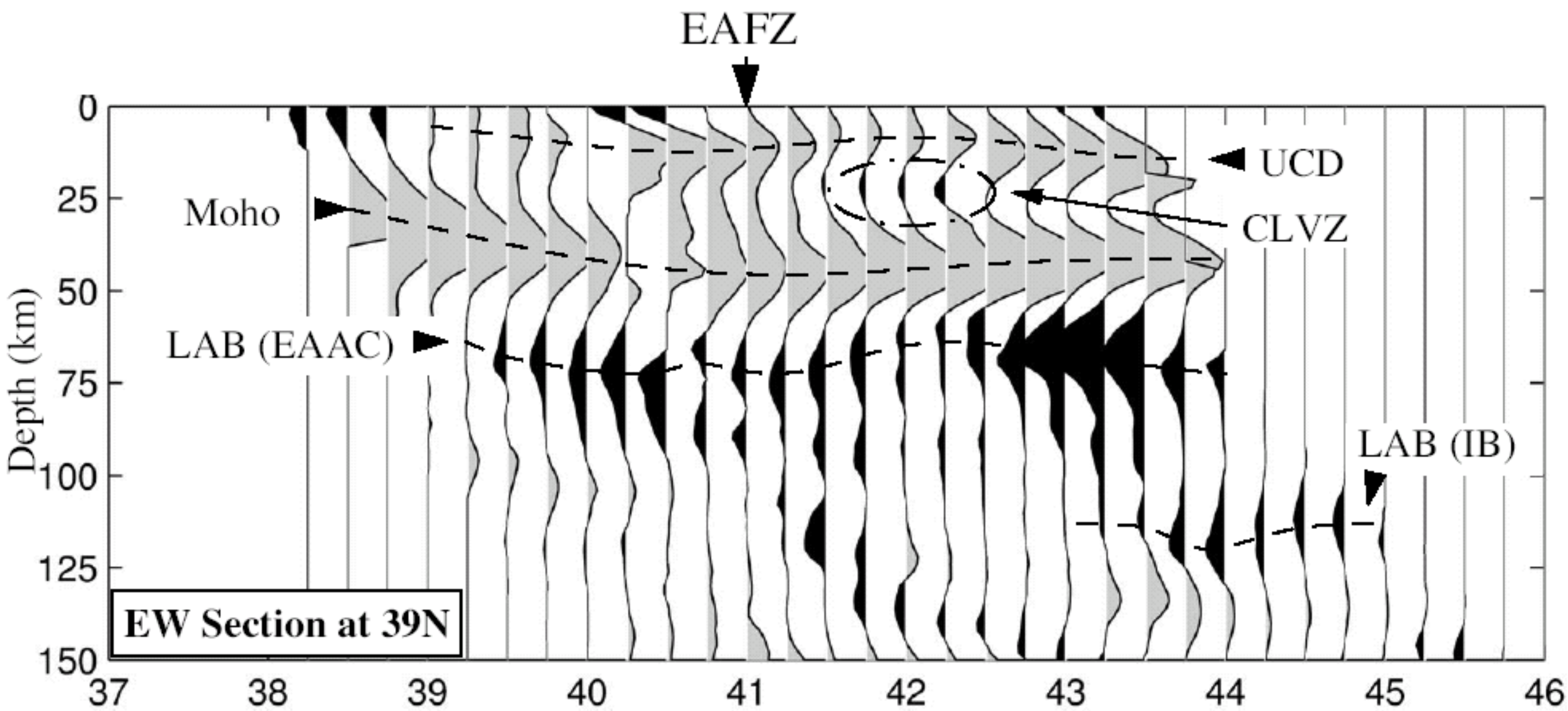

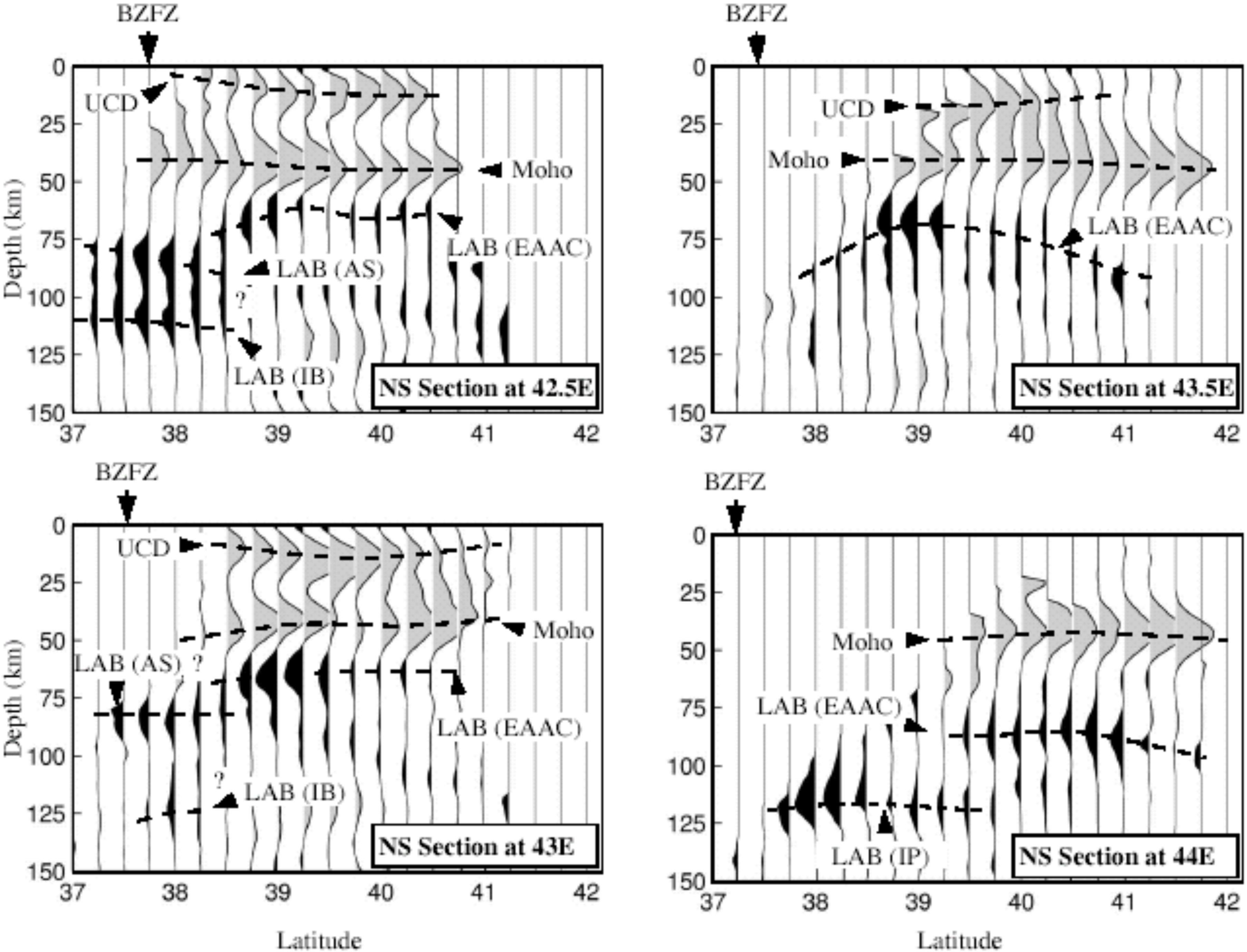

BZFZ
UCD
Moho
LAB (EAAC)
LAB (AS)
?
LAB (IB)
NS Section at 42.5E
Depth (km)
BZFZ
UCD
Moho
LAB (EAAC)
NS Section at 43.5E
BZFZ
UCD
Moho
LAB (AS)
?
LAB (EAAC)
?
LAB (IB)
NS Section at 43E
Depth (km)
Latitude
BZFZ
Moho
LAB (EAAC)
LAB (IP)
NS Section at 44E
Latitude